DISTINCT FUNCTIONS OF AUTOPHAGY KINASES ULK1 AND ULK2 IN ADIPOGENESIS AND ADIPOCYTE METABOLISM

A DISSERTATION

SUBMITTED TO THE FACULTY OF THE GRADUATE SCHOOL

OF THE UNIVERSITY OF MINNESOTA

BY

SEUNG-HYUN RO

IN PARTIAL FULFILLMENT OF THE REQUIREMENTS

FOR THE DEGREE OF

DOCTOR OF PHILOSOPHY

Dr. Do-Hyung Kim, Advisor

December 2011

Acknowledgements

I would like to express my appreciation for my advisor, Dr. Do-Hyung Kim for allowing me to work and study in his wonderful lab. I would not have been able to finish my Ph.D. degree without his support and mentoring. He was always encouraging and guided me to become a creative scientist. I wish him prosperous on his research as a generous professor.

I also would like to thank former and current Kim lab members. Emilie Vander haar, Seong-il Lee, Sricharan Bandhakavi, Young-Mi Kim, Changbong Jun, James Hegg, So-Yon Woo, Dong-Hwan Kim, Chang Hwa Jung, Jing Cao, Boah Vang, Neil Otto, Young Sung Yun, Minchul Seo for their help, support and friendship in the lab.

I would like to give my special thanks to Bernlohr lab members. Sandra Lobo, Jessica Curtis, Ann Hertzel, Brian Wiczer, Rocio Foncea, Brigitte Frohnert, Candace Gename for their helpful discussions and let me freely use their experiment facilities. I would like to express my tremendous appreciation for Wendy Hahn. She was teaching me all the mouse work and tissue preparations which were indispensible techniques for my future career. I would like to thank Xin Xu and Dr. Edgar Arriaga in Chemistry department for their help and discussion on mitochondria work.

I would like to thank my committee, Drs. Anja Bielinsky (DGS), Hiroshi Matsuo, Vivian Bardwell for advising me for preliminary exam. Drs. Timothy Griffin (Chair), David Bernlohr, Alex Lange, Thomas Neufeld for their advise and comments on my research until graduation.

Finally, I owe my special appreciation to my family - my Mother, Father and only younger brother Seung-Pyo in Korea for their love and prayer on my peaceful life and success in USA. I love you so much.

I am indebted to my prayer supporters - Pastor. Jong Dae Eun, Wonju Jeon, Jung kyoon Choi, Seongwon Cha, Dae Hoon Lee, Chang Eui Seo, Jae-Hyun Kim, Sunhee Choi, Suhyoung Sim from Daeduk Hanbit Presbyterian Church in Daejon, Korea. The prayer supporters in Stadium Village Church and Korean Presbyterian Church in Minnesota, USA - Pastors. Lowell Busman and Kathleen Macosko, Chris Macosko, Donny Choi, John Lee, Min Young Cha, Pastor. Sun Woo Kang, Sam Lee, and all the Korean small group members. I love you all.

Dedication

This dissertation is dedicated to my Lord and Savior, **Jesus Christ**. You are the only reason for my life journey to honor your glory. You have stood together with me not only on joyful times but also on very hard times all through my life. I love you above all, forever.

Abstract

Autophagy, the catabolic process through which intracellular constituents are degraded in the lysosome under nutrient starvation or stress, has gained growing attention in the field of diabetes and obesity (Goldman S 2010; Ost A 2010; Beau I 2011; Kovsan J 2011). Despite the fundamental cellular function of autophagy in maintaining cellular energy homeostasis and survival under nutrient- or energy-deprived conditions and stress, the role of adipose autophagy in metabolism and metabolic diseases remains largely unknown. The goal of my study has been to better understand the function of autophagy in adipogenesis and in the regulation of adipocyte metabolism. My study has been focused on defining the role of ULK1 (Unc-51 like kinase 1, mammalian homolog of Atg1, hATG1) and its homologue ULK2 in the regulation of adipogenesis, metabolism and mitochondrial functions in adipocytes. ULK1 and ULK2 are key regulators of autophagy induction in mammalian cells (Kundu M 2009; Chang YY 2009; Ganley IG 2009; Hosokawa N 2009; Jung CH 2009). Knockdown of ULK1 or ULK2 inhibited autophagy in 3T3-L1 adipocytes, suggesting that they play important roles in autophagy in adipocytes. The knockdown experiment also revealed that ULK1 and ULK2 share key functions in lipolysis, mitochondrial respiration and protection of cells against oxidative stress. Despite these shared functions, their knockdown had different or even opposing effects on several metabolic parameters. Knockdown of ULK1 raised PPAR-γ level, facilitated differentiation of 3T3-L1 cells, increased the levels of GLUT4, insulin receptor β (IRβ) and insulin receptor substrate-1 (IRS-1), and insulin-stimulated glucose uptake, and reduced fatty acid oxidation. By contrast, knockdown of ULK2 had opposite or no significant effects on these parameters. Through knocking down both ULK1 and ULK2, we found that ULK2 has a dominant effect over ULK1 in the regulation of adipogenesis. These results demonstrate that ULK1 and ULK2 have distinct functions in the regulation of adipogenesis and adipocyte metabolism, and that ULK2-dependent autophagy appears to be important for adipogenesis.

Table of Contents

List of Tables

List of Figures

List of Abbreviations

1. Autophagy and mTOR pathway

AMPK, 5′-AMP-activated protein kinase;

Atg, Autophagy-related gene;

FIP200, Focal adhesion kinase (FAK) family interacting protein of 200 kDa;

LC3, Microtubule associated protein 1B light chain 3;

LKB1, Serine/Threonine protein kinase 11, STK11;

Mitophagy, Mitochondria selective autophagy;

mTOR, Mammalian target of rapamycin;

mTORC, mTOR complex;

p62/SQSTM1, Ubiquitin-binding protein p62/sequestosome 1;

PKB, Protein kinase B, also known as Akt;

Raptor, Regulatory associated protein of mTOR;

STK36, Serine/Threonine kinase 36, also known as FUSED;

ULK, UNC-51-like kinase;

2. Adipogenesis and insulin signaling

BAT, Brown adipose tissue;

CEBP-α, CCAAT/enhancer binding protein-α;

DEX, Dexamethasone;

EWAT, Epididymal white adipose tissue;

FFA, Free fatty acid;

GAPDH, Glyceraldehyde-3-phosphate dehydrogenase;

GLUT, Glucose transporter;

HFD, High fat diet;

Ins, Insulin;

IRβ, Insulin receptor β;

IRS, Insulin receptor substrate;

LD, Lipid droplet;

MIX, Methylisobutylxanthine;

PPAR-γ, Peroxisome proliferator-activated receptor-γ;

SREBP-1, Sterol regulatory element-binding protein-1;

TZD, Troglitazone;

3.Mitochondria function and energy metabolism

ACC, Acetyl CoA carboxylase;

COXII, Mitochondrial cytochrome c oxidase II;

CytC, Cytochrome C (mitochondrial);

EM, Electron microscopy;

eNOS, Endothelial nitric oxide synthase;

ETC, Electron transport chain;

FASN, Fatty acid synthase;

FABP, Fatty acid-binding protein, also known as aP2;

FATP, Fatty acid transport protein;

FCCP, Carbonyl cyanide 4-(trifluoromethoxy) phenylhydrazone;

PGC-1α, Peroxisome proliferator activated receptor gamma coactivator-1 α;

TAG, Triacylglyceride;

Tfam, Transcription factor A, mitochondrial;

UCP2, Uncoupling protein 2;

VDAC, Voltage-dependent anion channel;

4.Oxidative stress, pro-inflammation and apoptosis pathway

4-HNE, *trans*-4-*hydroxy*-2-nonenal;

NF-kB, Nuclear factor-kappa B;

NQO-1, Quinine oxido-reductase-1;

NRF, Nuclear respiratory factor;

p-38 MAPK, p-38 mitogen-activated protein kinase;

ROS, Reactive oxygen species;

TNFα, Tumor necrosis factor α;

TUNEL, Terminal deoxynucleotide transferase dUTP nick end labeling;

CHAPTER 1 : Introduction

1.1. Adipose tissue - a central organ responsible for energy metabolism and homeostasis in the body

Adipose tissue plays a key role in maintaining energy homeostasis in our body by releasing or storing lipids in response to the body energy demand and food uptake (Fig. 1). Adipose tissue takes up fatty acids and coverts them into triacylglycerides (TAG), the form of lipid stored in the tissue. Under starvation or high energy demand, TAG is converted into fatty acids that are secreted for usage in other tissues. TAG can also be oxidized in mitochondria to produce heat instead of ATP thereby maintaining the body temperature (De Pauw A 2009; Bournat JC 2010; Wang CH 2010). The white adipose tissue (WAT) is responsible for storage and release of lipids, whereas the brown adipose tissue (BAT) is responsible for maintaining the body temperature homeostasis (Camp HS 2002; Rosen ED 2006; Trayhurn 2007). Accumulation of fatty acids in other tissues due to metabolic problems in adipose tissue can cause hypertension, atherosclerosis, obesity and insulin resistance (Camp HS 2002; Gustafson 2010; Marcelin G 2010; Achike FI 2011)

Adipose tissue also takes up glucose in response to insulin and converts it into lipid for storage thus playing an important role in maintaining glucose homeostasis in our body (Saltiel AR 2001; Rosen ED 2006; Trayhurn 2007). Although adipose tissue control

small portion up to 15% of glucose in the circulation, both too high fat (obesity) and too little fat (lipodystrophy) can cause insulin resistance. This implies that glucose regulation by adipose tissue is important for glucose homeostasis in the body (Kahn 1996; Rosen ED 2006). Thus, insulin-responsive glucose uptake by adipose tissue is important for our body metabolism. Supporting this notion, insulin resistance developed in the mice in which GLUT4, the glucose transporter responsible for insulin-stimulated glucose uptake in adipocytes, is deficient in adipose tissue (Abel ED 2001).

Adipose tissue is important not only for energy homeostasis or the body temperature maintenance but also for the secretion of cytokines (called adipokines) or hormones that control inflammatory response in the tissue. Adiponectin, visfatin, and omentin are some examples of adipokines that act as anti-hyperglycaemic factors to suppress high blood glucose levels. Resistin, TNFα, and interleukin-6 (IL-6) are other types of adipokines that act as pro-hyperglycaemic factors to raise blood glucose levels (Rosen ED 2006; Trayhurn 2007). Some of adipokines are propagated to peripheral tissues and the brain to have a global effect on the body metabolism. An example is leptin. Leptin is propagated to the hypothalamus in the brain thus affecting the appetite.

Given the key functions of adipose tissue in energy homeostasis and in the development of many metabolic diseases, it is important to understand better how adipose tissue functions and metabolism are regulated and how its function is disrupted in the metabolic disease states. Many of the key metabolic processes conducted by adipocytes

are dependent upon mitochondrial functions (Lowell 2005; De Pauw A 2009; Bournat JC 2010; Wang CH 2010; Achike FI 2011). In the following section, I will briefly describe the functions of mitochondria in adipocytes and how my study is related to mitochondrial functions.

1.2. Mitochondria - the key organelle for energy metabolism in adipocytes

Mitochondria are the key cellular organelle responsible for production of energy (ATP), thus its function is crucial for cell growth, survival and other basic cellular functions (Fig. 2). Mitochondria in adipocytes are important given their key role in metabolizing glucose and fatty acids through the TCA cycle and the oxidative phosphorylation (Boudina S 2005; Cheng Z 2010). Mitochondrial dysfunction is closely linked to obesity and insulin resistance (Bournat JC 2010; Wang CH 2010). Mitochondria are important not only for ATP production and energy metabolism but also for apoptotic process and cellular oxidative stress response. Mitochondria play key role in apoptosis through releasing cytochrome c. Mitochondria are the main source of the reactive oxygen species (ROS) in cells (Ueda S 2002; De Pauw A 2009; Bournat JC 2010; Circu ML 2010; Hamanaka RB 2010; Rigoulet M 2011).

Mitochondrial dysfunction is closely linked to obesity and insulin resistance (Bournat JC 2010; Wang CH 2010). Increased ROS, protein oxidation and cell death can be caused by dysfunctional mitochondria in obesity and type 2 diabetes (Lowell 2005; Grimsrud PA 2007; De Pauw A 2009; Wang CH 2010).

ROS are short-lived and highly reactive molecules including superoxide, hydroxyl radicals and peroxides. They are byproducts of oxygen consumption and oxidative phosphorylation in mitochondria. Oxidative stress or TNFα can induce mitochondrial

damages which can increase the production of more ROS and protein oxidations such as carbonylation (Curtis JM 2010). Thus, clearance of damaged mitochondria is important to suppress the accumulation of oxidative stress in adipocytes.

Damaged mitochondria are known to be degraded selectively through a cellular process called autophagy that is the main subject of my thesis work. Given the appreciated importance of clearance of damaged mitochondria, it is considered to be important to better understand the role of autophagy in the regulation of oxidative stress response and metabolism in adipocytes. The following chapter will introduce the general functions of autophagy and the currently-known functions of autophagy in adipocytes.

1.3. Autophagy in adipocyte metabolism

Autophagy is an evolutionarily conserved process through which cytoplasmic components are captured into double-membrane structures called autophagosome and degraded in the lysosome (Fig. 3) (Bursch W 2000; Levine B 2008; Mizushima N 2008; Singh R 2009). Although the origin of autophagosomal membrane remains unclear, several reports demonstrated that the membrane originates from endoplasmic reticulum (ER), Golgi, or mitochondria membrane (Weidberg H 2011). There are two types of autophagy; macroautophagy, and selective autophagy (Levine B 2008; Mizushima N 2008). Macroautophagy is a non-selective process through which intracellular components are randomly captured by autophagosome and degraded in the lysosomes during nutrient starvation. This process is believed to be important for cell survival under starvation or stress or for cellular differentiation. On the other hand, selective autophagy occurs to target and degrade specific cellular components and organelles (Fig. 4). Mitophagy is an example of selective autophagy through which damaged mitochondria are selectively recognized by autophagosomes and degraded in the lysosomes.

Autophagy has gained growing attention in the field of diabetes and obesity as a potential contributing factor to insulin resistance due to its key role in maintaining cellular energy homeostasis and survival and removing damaged mitochondria under nutrient- or energy-deprived states and stress (Goldman S 2010; Ost A 2010; Beau I

2011; Kovsan J 2011). Recent studies have shown that autophagy in adipose tissue is perturbed in obesity and insulin resistance state. Inhibition of autophagy by 3-methyl adenine treatment prevented insulin receptor degradation induced by ER stress in adipose tissue from obese mice (Yorimitsu T 2006; Zhou L 2009; Shimada Y 2011). Autophagy was also up-regulated in adipose tissue of obese persons and type 2 diabetes patients (Ost A 2010; Beau I 2011; Kovsan J 2011).

Recent studies have revealed that adipogenesis is dramatically suppressed when a key autophagy gene Atg5 is deficient in mouse embryonic fibroblasts (MEFs) (Baerga R 2009). Consistent with the results from cultured adipocytes, the adipose-specific deletion of Atg7 resulted in lean mice and enhanced insulin sensitivity in the body (Singh R 2009; Zhang Y 2009). The Atg7 KO mice showed reduction in the mass of WAT and an increase in the mass of BAT. WAT in Atg5 or Atg7 KO mice contained adipocytes that have the feature of brown adipocytes with an elevated rate of fatty acid oxidation and a higher mitochondrial content (Singh R 2009).

Although these studies have provided important insight into the role of autophagy in adipose development, the metabolic changes in Atg5- or Atg7-ablated mice are more likely attributed to the increase in BAT mass during the animal development. It remains unclear how autophagy contributes to metabolic disease states that are caused by metabolic changes or stress at adults after development. Furthermore, a recent study revealed that autophagy can occur in a manner independent of Atg5/Atg7 while still

depending on ULK1(Nishida Y 2009). Thus, it is necessary to study functions of ULK1 and other autophagy proteins to better understand the roles of adipocyte autophagy in metabolism.

1.4. ULK – the key protein kinase in the autophagy pathway

ULK1 is a Ser/Thr kinase that plays a key role in inducing autophagy in response to starvation in a variety of cell types (Chang YY 2009; Hosokawa N 2009; Jung CH 2009; sokawa N 2009; Dunlop EA 2011) (Fig. 5). The human genome has five ULK1 homologues, which are ULK1, ULK2, ULK3, ULK4 and STK36 (Ser/Thr kinase 36) (Jung CH 2010; N. 2010) (Fig. 6). Among them, only ULK1 and ULK2 have been shown to regulate autophagy in various cell types (Ganley IG 2009; Hosokawa N 2009; Jung CH 2009; Kundu M 2009; Egan DF 2011). ULK1 and ULK2 form two distinct protein complexes by interacting with Atg13, focal adhesion kinase family interacting protein of 200 kD (FIP200), and Atg101 (Fig. 5) (Chan 2007; Hara T 2008; Ganley IG 2009; Hosokawa N 2009; Hosokawa N 2009; Jung CH 2009; Mercer CA 2009; Jung CH 2011). ULK1 and ULK2 show 52% of identity in the amino acid sequences (Jung CH 2010). Although ULK1 is a key molecule in the autophagy pathway, mice lacking ULK1 in the whole body were viable without showing any apparent developmental defect (Kundu M 2009). This might be due to a compensatory function of ULK2 for the loss of ULK1.

ULK1 is phosphorylated by mTORC1 (mTOR complex 1) and AMPK (5’ AMP-activated protein kinase), the key cellular nutrient and energy sensing kinases (Egan D 2011; Egan DF 2011; Kim J 2011). mTORC1 and AMPK have opposite effects on ULK1 activity. AMPK phosphorylation of ULK1 stimulates ULK1 to trigger autophagy,

whereas mTORC1 phosphorylation of ULK1 prevents AMPK from binding to ULK1 thus inhibiting autophagy induction (Kundu M 2009). Thus, ULK1 is a key molecule that integrates and transmits signals from mTORC1 and AMPK to the autophagy machinery (Fig. 7). ULK1 also plays a critical role in the regulation of autophagic degradation of mitochondria (mitophagy) in maturing reticulocytes, hepatocytes, and fibroblasts (Kundu M 2009; Egan DF 2011).

The macroautophagy or mitophagy induced by ULK1/2 complex may degrade defective mitochondria and other cellular structures so that it may contribute to abrogate metabolic problems caused by ROS. Oxidative stress such as ROS and mitochondrial dysfunction can be caused by alteration in lipid metabolism (De Pauw A 2009; Bournat JC 2010). Saturated FFA may alter lipid storage and balance in the form of TAG in adipocytes, which can significantly deteriorate the metabolic function of mitochondria. Mitochondrial dysfunction and increased glucose utilization is the featured phenotypes of tumor cells known as Warburg effect (Gogvadze V 2010). We assume that glucose transport and glycolysis may be altered as a consequence of imbalance in lipid metabolism and mitochondria dysfunction in adipocytes (Fig. 7). Furthermore, molecular mechanism of how oxidative stress and mitochondria dysfunction can affect the mTOR/AMPK/ULK1-regulated autophagy remains unclear (Fig. 7).

ULK1 and ULK2 were shown to inhibit mTORC1 signaling (Scott RC 2007; Dunlop EA 2011; Jung CH 2011), which was not the case with Atg5 or other autophagy genes.

ULK1 binds to AMPK and phosphorylates AMPK (Löffler AS 2011). Thus, ULK is a unique component in the autophagy pathway that functionally interacts with AMPK and mTORC1, which regulate mitochondrial biogenesis, adipogenesis and metabolism in adipocytes. Based on this knowledge, it is important to investigate the role of ULK in adipocytes. Given that mTORC1 signaling is known to be important for adipogenesis (Zhang HH 2009), Whether ULK1 contributes to adipogenesis through altering mTORC1 signaling is an interesting question.

1.5. The overall scope and the central hypothesis of my study

Given the key functions of ULK1 in the regulation of autophagy and mitochondrial clearance, this kinase must play an important role in the regulation of adipocyte metabolism. I hypothesize that ULK1 may regulate adipogenesis and adipocyte metabolism through altering mTORC1 signaling and mitochondria function and metabolism. Based on the known and anticipated functions of ULK1, I hypothesized that ULK1 may have critical roles in the regulation of adipocyte metabolism and mitochondria functions through the autophagy process. To test the hypothesis, I first examined the levels of autophagy-related proteins and autophagy activity in adipose tissue of lean and obese mice to investigate how autophagy is affected by high fat diet. Next, 3T3-L1 adipocytes were stably transduced by shRNA specific to ULK1 or ULK2. As controls, 3T3-L1 adipocytes were transduced by shRNAs for GFP (green fluorescence protein) or a scrambled sequence. For comparison with other autophagy gene, Atg5-silenced 3T3-L1 adipocytes were also prepared. Using the shRNA-transduced adipocytes, I assayed autophagy, adipogenesis, insulin signaling, glucose and lipid metabolism, mitochondrial function and apoptotic cell death. By comparing metabolic assays in each ULK1, ULK2 or Atg5-silenced adipocytes, I have determined the unique and shared functions of ULK1 and ULK2 in adipogenesis and adipocyte metabolism. Knowing that ULK2 is a closely related homologue of ULK1, my study also investigated the functions of ULK2 along with ULK1 in the regulation of adipogenesis and adipocyte metabolism.

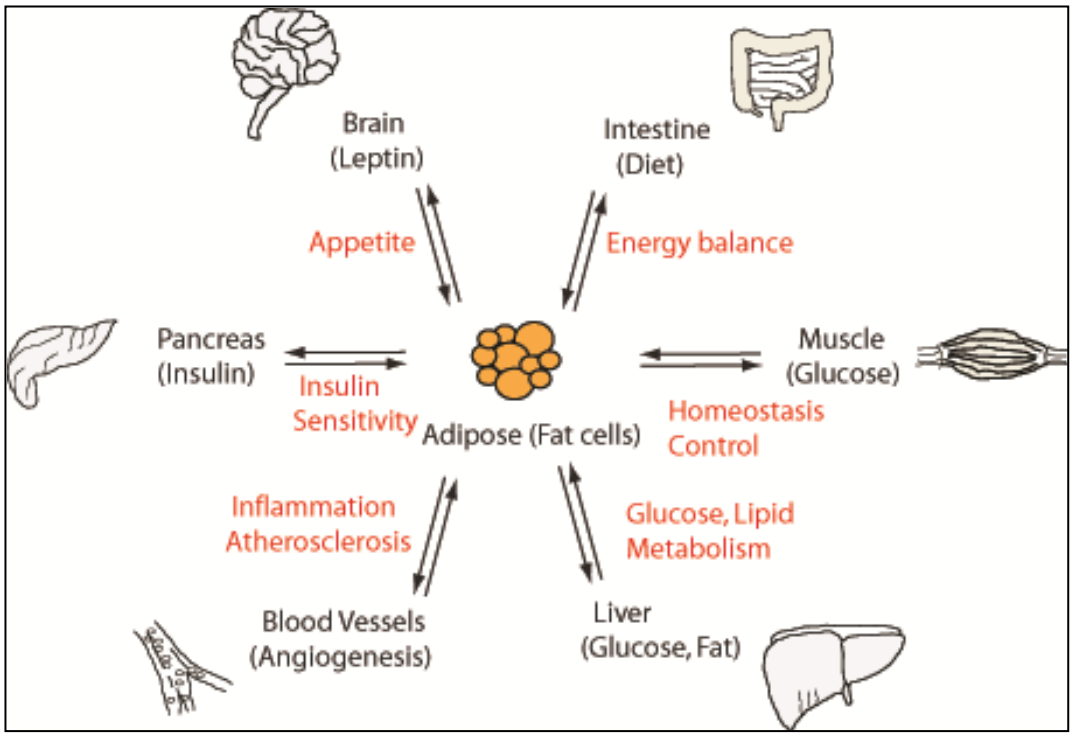

Figure 1. Adipose tissue is a central organ that regulates energy metabolism and homeostasis in the body. Adipose tissue plays a central role in maintaining energy homeostasis in our body by storing or releasing lipids, uptaking glucose, and secreting cytokines thereby affecting insulin sensitivity and glucose and lipid metabolism and homeostasis in other peripheral tissues.

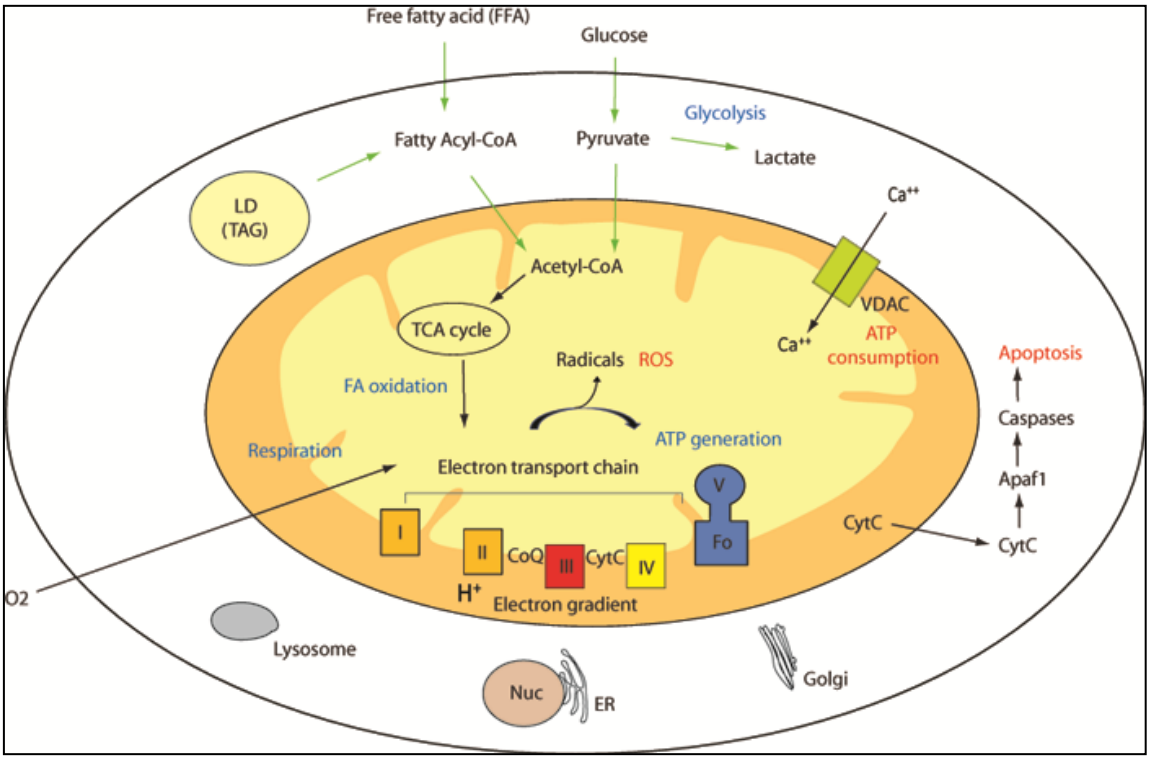
Free fatty acid (FFA)
Glucose
Glycolysis
Fatty Acyl-CoA
Pyruvate
Lactate
LD
(TAG)
Ca++
Acetyl-CoA
VDAC
TCA cycle
Ca++
ATP
consumption
Apoptosis
Radicals ROS
FA oxidation
Caspases
ATP generation
Respiration
Electron transport chain
Apaf1
V
I
II
CoQ
III
CytC
IV
Fo
CytC
CytC
O2
H+
Electron gradient
Lysosome
Golgi
Nuc
ER

Figure 2. Mitochondria are the cellular organelle that plays key roles in energy metabolism in adipocytes. Mitochondria have molecular machinery which converts the chemical energy of fuels, such as carbohydrates and lipids into ATP. Pyruvate oxidation, the tricarboxylic acid (TCA) cycle, fatty acid beta oxidation, and oxidative phosphorylation through the electron transport chain are the processes that occur in mitochondria. Mitochondria dysfunction can cause an increase in ROS and oxidative stress, which can lead to insulin resistance in adipocytes (Lowell 2005; De Pauw A 2009; Bournat JC 2010). Mitochondria also consume ATP by mediating metabolite (i.e. Ca^{++}) transport through voltage-dependent anion-selective channel (VDAC). This metabolite transport is important for maintaining cellular metabolite homeostasis, protection against oxidative stress, and regulation of apoptotic cell death (Shoshan-Barmatz V 2010). When mitochondria are damaged or treated with TNFα, mitochondria release cytochrome C (CytC), which induces apoptotic cell death signaling through apoptotic peptidase activating factor 1 (Apaf) 1 and caspases (Circu ML 2010). LD, lipid droplets; Nuc, nucleus.

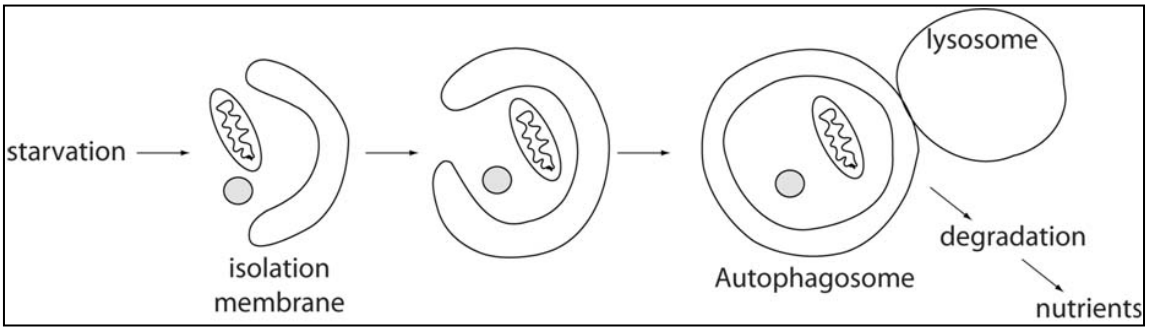

Figure 3. Scheme for autophagy process induced by starvation. Autophagy is an evolutionarily-conserved catabolic process induced by starvation through which cellular constituents and damaged macromolecules and organelles are degraded in the lysosome.

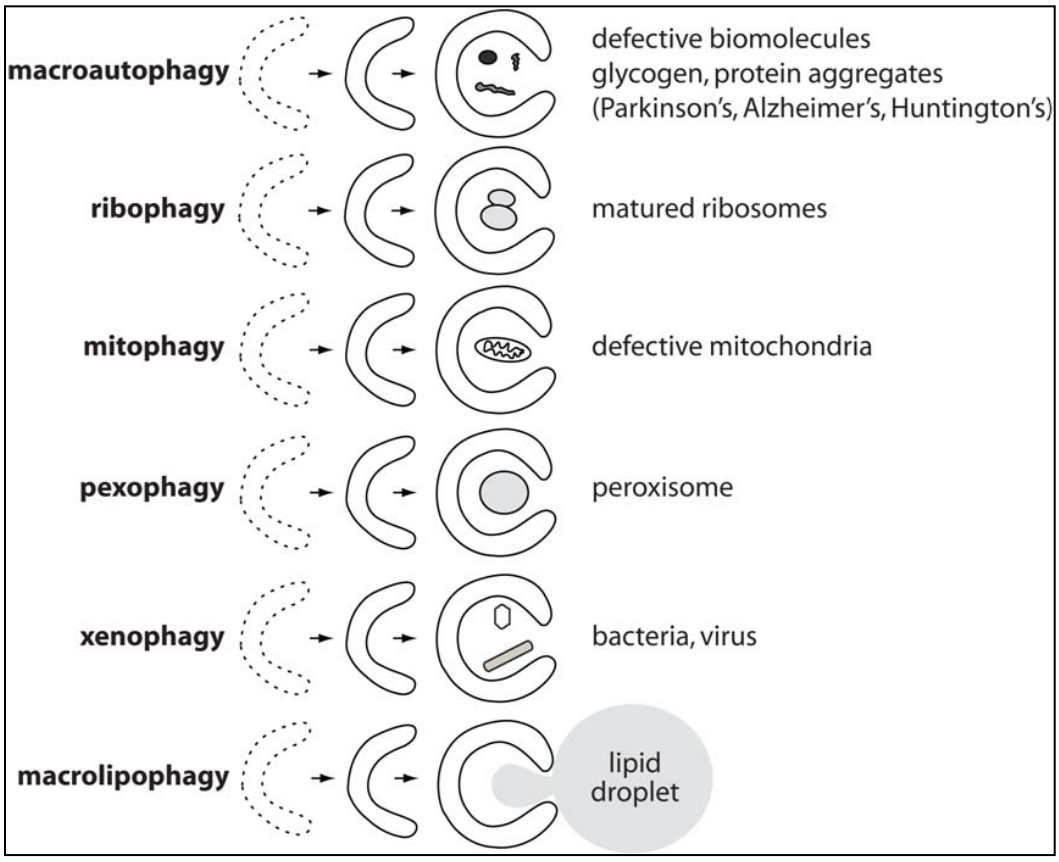

Figure 4. Types of autopahgy occurring in mammalian cells. Macroautophagy is a type of autophagy that randomly engulfs cytoplasmic compartments and degrades them during starvation, On the other hand, selective autophagy is specific to ribosomes, mitochondria, peroxisome, bacteria, or viruses for their degradation. Lipid droplets can be degraded by autophagy in starvation, which was firstly described in hepatocytes (Singh R 2009), and named macrolipophagy.

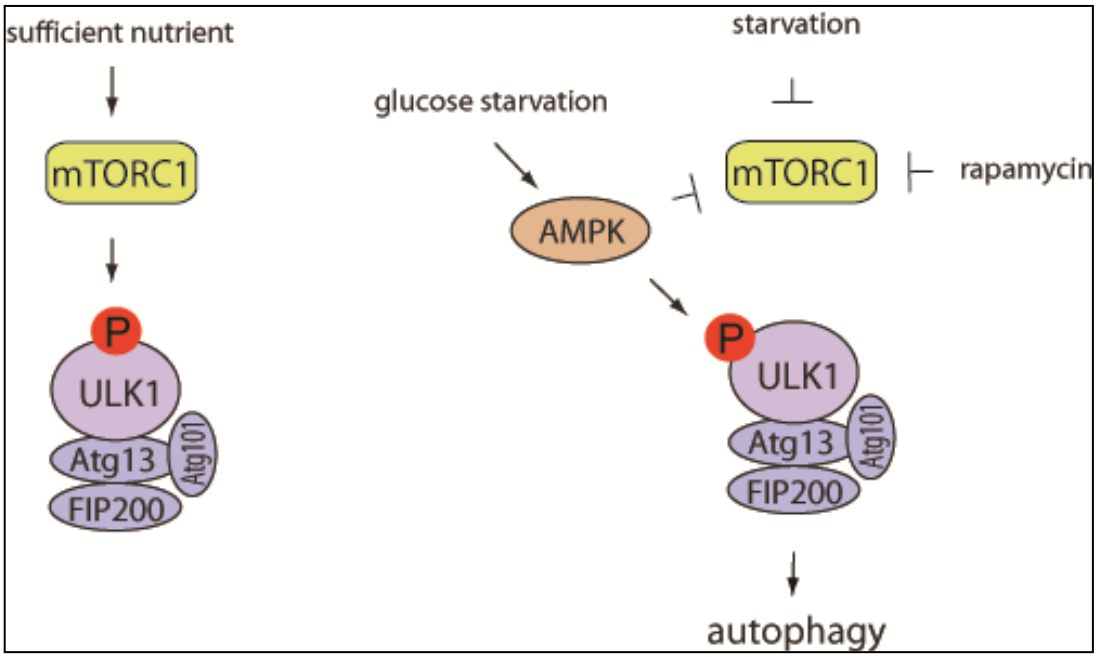

Figure 5. ULK1 is the key protein kinase in the autophagy pathway. ULK1 is a Ser/Thr kinase that plays a key role in inducing autophagy in response to starvation in mammalian cells. ULK1 integrates and transmits signals from mTORC1 and AMPK to the autophagy machinery (Jung CH 2009; Egan DF 2011; Kim J 2011). Under sufficient nutrient condition, active mTORC1 phosphorylate ULK1 and inhibit autophagy induction. Under starvation condition, mTORC1 is inactive and ULK1 can induce autophagy. AMPK also phosphrylate ULK1 and activate autophagy induction in glucose starvation condition.

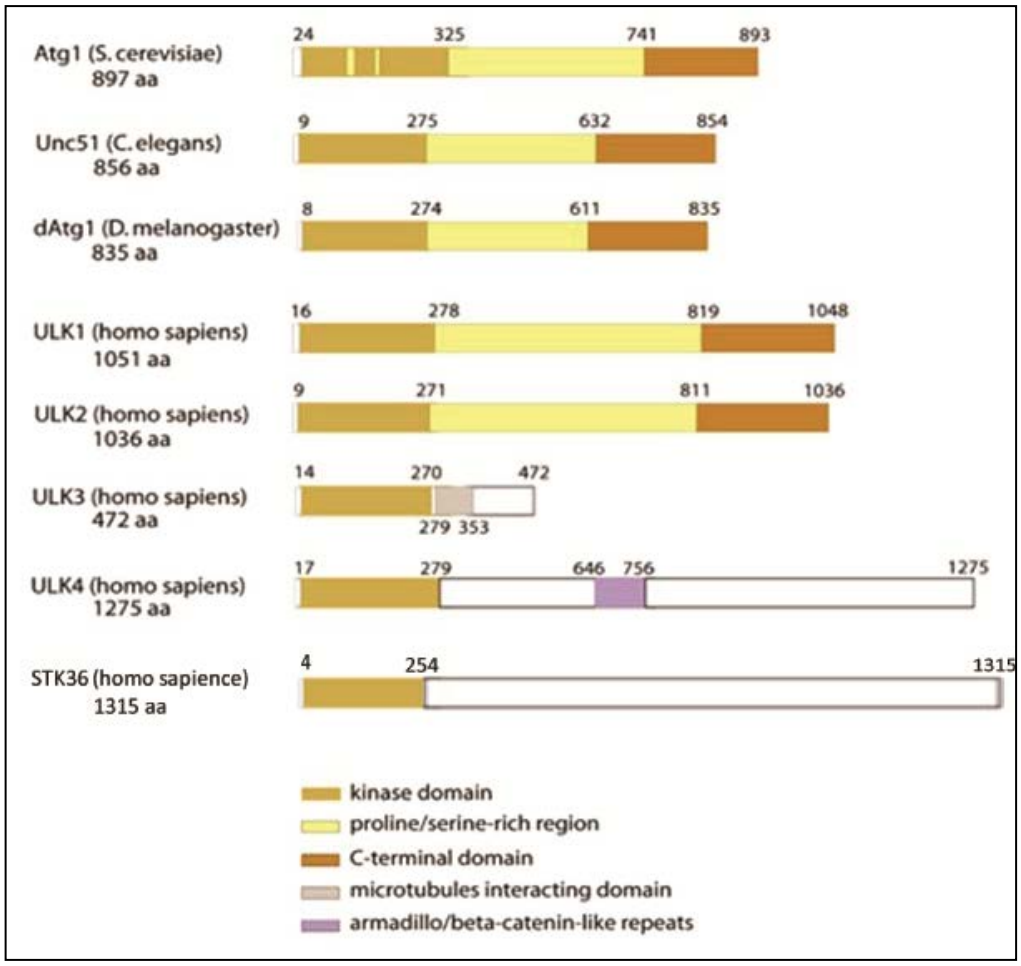

Figure 6. There are five isoforms of ULK in mammals. Schematic representation of domain structures of the five ULK isoforms and their homologues in yeast, *C. elegans* and *Drosophila*. ULK1 and ULK2 share 52% identity in their amino acid sequences.

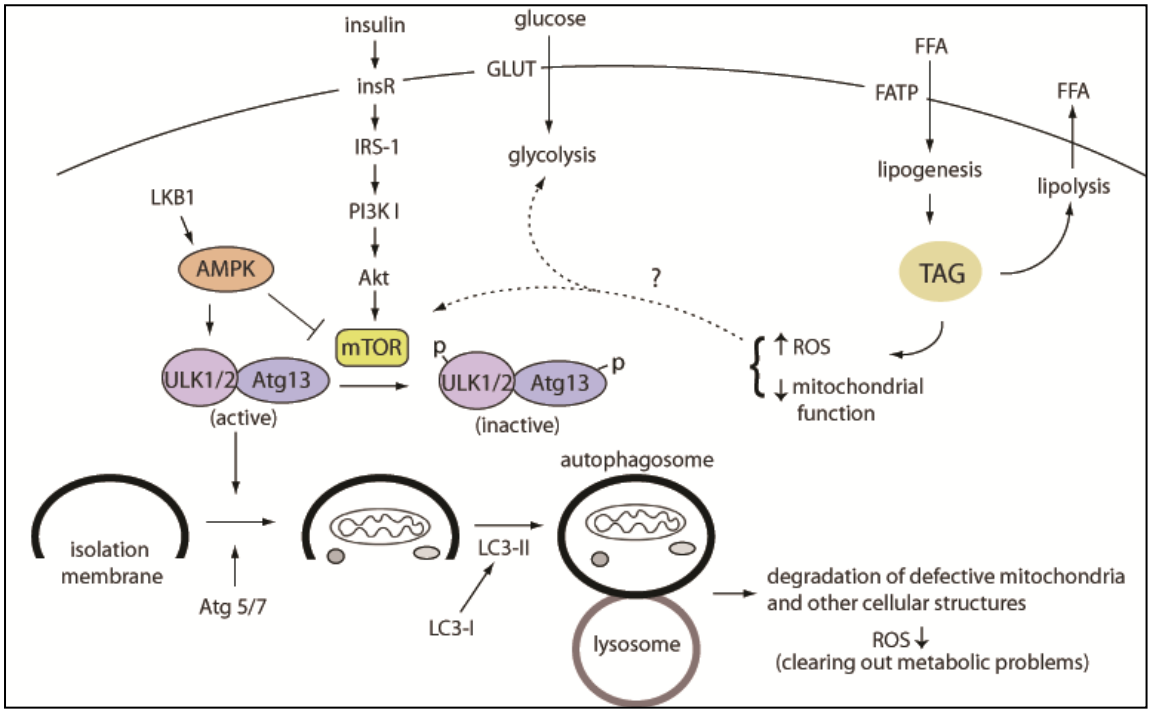
insulin
glucose
FFA
insR
GLUT
FATP
FFA
IRS-1
glycolysis
lipogenesis
lipolysis
LKB1
PI3K I
AMPK
Akt
?
TAG
mTOR
↑ ROS
↓ mitochondrial function
p
ULK1/2
Atg13
p
ULK1/2
Atg13
(active)
(inactive)
autophagosome
isolation membrane
LC3-II
Atg 5/7
LC3-I
lysosome
degradation of defective mitochondria and other cellular structures
ROS↓
(clearing out metabolic problems)

Figure 7. Regulation of autophagy and lipid metabolism in adipocytes. ULK1/2 complex is regulated by mTOR and is important for autophagy induction (Jung CH 2009). When ATP level is low or glucose is depleted, LKB1 phosphorylates and activated AMPK (Shaw RJ 2004). Activated AMPK phosphorylates ULK and induces macroautophagy or mitophagy (Egan DF 2011; Kim J 2011). When the lipid metabolism is altered in adipocytes, the ROS level may increase along with mitochondria dysfunction. Glucose transport and glycolysis process can be altered as a consequence of imbalance in lipid metabolism. The macroautophagy or mitophagy induced by ULK1/2 complex may degrade defective mitochondria and other cellular structures so that it may contribute to reduction in metabolic problems such as ROS.

CHAPTER 2 : ULK1 and ULK2 are important for adipocyte autophagy

Introduction : Previous studies indicated that autophagy is important for adipogenesis and adipose metabolism (Baerga R 2009; Singh R 2009; Zhang Y 2009). In this chapter, my study aimed to determine how nutrient conditions affect the autophagy activity. To achieve this goal, I performed experiments to monitor the autophagy activities in adipose tissue in mice subjected to high fat or low fat diets and adipocytes treated with starvation-mimicking conditions in cell culture. Autophagy activity was assayed by multiple approaches including analysis of LC3 processing, the expression level of p62, LC3-positive autophagosomal puncta formation, and EM images of autophagosomes. These assays showed that autophagy in adipose tissue and adipocytes in cell culture is perturbed in response to the nutritional treatments. Using adipocyte cell culture model, I found that ULK1 and ULK2 are important for basal and rapamycin-induced autophagy in adipocytes. These results are described in detail in the following sections.

2.1. Autophagy is up-regulated in adipose tissue from mice fed with high fat diet.

Previous studies in adipose tissues in Atg5 or Atg7 deleted mice revealed that autophagy regulates adipogenesis and lipid metabolism (Baerga R 2009; Singh R 2009; Zhang Y 2009). Assuming that various nutrient conditions may reciprocally affect the autophagy activity and its regulation in adipose tissues, I asked how the activity of autophagy in adipose tissue is affected by diet in mice. To address the question, I designed two groups of mice with standard chow diet and high fat diet which represent nutritional status regulating autophagy activity differently in the body.

Male mice strain C57BL/6J were fed normal chow (~ 4% fat by weight, Teklad) or high fat diet (~35 % fat by weight, F3282, BioServ) at weaning (Surwit RS 1988). Mice were housed on a 12-h light/dark cycle and fed ad libitum with continual access to water. At 12 weeks of age, they were weighing 34-49 g and 26-33 g, respectively. Each group of mice were fasted for 4 h and euthanized by carbon dioxide. Epididymal white adipose tissue (EWAT) from CHOW low fat and high fat mice were isolated and proteins were extracted from the prepared tissue. The expression levels of key autophagy proteins such as ULK1, Atg5 and LC3 as well as key components in the insulin signaling pathway such as IRβ, IRS-1 and p-S6K1 were analyzed by Western blotting.

We observed that microtubule-associated protein 1B light chain 3 (LC3)-I conversion to LC3-II, a form of LC3 modified with phosphatidylethanolamine at C-terminus, was

markedly increased by three fold in adipose tissue from high fat diet mice (Fig. 8A and B). LC3-II is associated with autophagolysosomes and known to reflect autophagy activity in mammalian cells (Klionsky DJ 2008; Klionsky DJ. 2008). The protein levels of ULK1 and Atg5 were not significantly changed by high fat diet (Fig. 8A and C), indicating that high fat-diet induced autophagy occurs without needing a change in the level of Atg5 and ULK1. Consistent with previous reports (Um SH 2004), high fat diet (HFD) enhanced the phosphorylation of S6K1 while reducing the levels of IRβ and IRS-1 (Fig. 8A). A key finding from this experiment is that autophagy activity in adipose tissue is responsive to the diet of mice. This result implies that adipocyte autophagy might play an important role for adipocytes to appropriately respond to high fat diet or metabolic stress. This result is consistent with the overall hypothesis of my study.

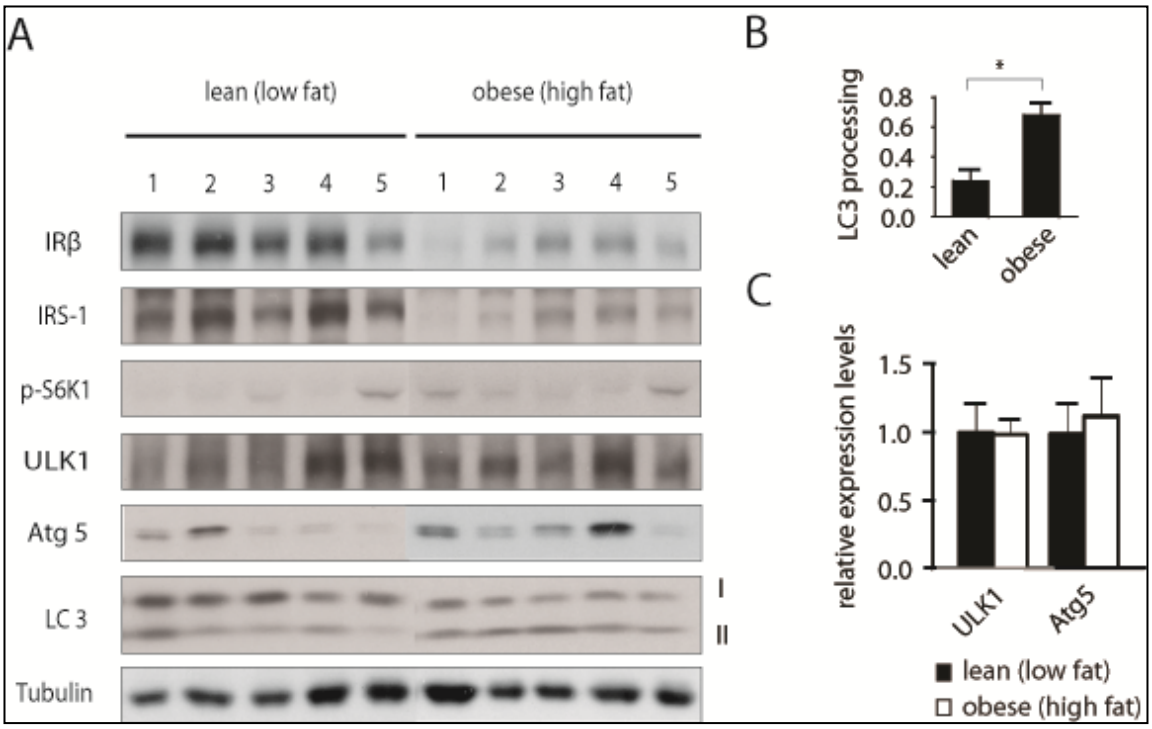

Figure 8. Autophagy is increased in adipose tissue from high fat diet mice. (A) EWAT from low fat or high fat diet mice was lysed in RIPA buffer. The levels of the indicated proteins in tissue extracts were analyzed by Western blotting. (B) Quantitative analysis of LC3-II versus LC3-I on the blot from (A). Values are mean ± standard deviation (std.) *, $p < 0.05$. (C) Quantitative analysis of ULK1 and Atg5 levels. Values are mean ± std. Detailed procedures are described in Materials and Methods section.

2.2. ULK1 and ULK2 are important for basal and rapamycin-induced autophagy in adipocytes.

In previous chapter, we observed HFD can trigger and increase autophagy activity in mouse adipose tissue. The increase in the autophagy activity in response to high fat diet supported my hypothesis that adipocyte autophagy might be important for adipocyte metabolism and metabolic problems associated with obesity. To determine the extent to which ULK1 and ULK2 affect autophagy in adipocytes, we transduced 3T3-L1 preadipocytes by shRNA specific to ULK1 and ULK2 and induced differentiation. As controls, we transduced 3T3-L1 cells by either scrambled or GFP shRNA. To compare with other autophagy genes, we also prepared Atg5-silenced 3T3-L1 cells. At day 10 after induction of differentiation, the transduced cells showed different extents of differentiation. To avoid the effects due to the different extents of differentiation on autophagy, we added troglitazone in the differentiation medium to equalize the extent of differentiation (Fig. 9). Troglitazone is a chemical that acts as a ligand for adipocyte differentiation (Tontonoz P 1994; Tontonoz P 2008; Curtis JM 2010). Basal autophagy was assayed by immunostaining LC3 (microtubule-associated protein 1 light chain 3)-positive autophagosomal puncta. Knockdown of ULK1, ULK2 or Atg5 significantly suppressed the formation of LC3-positive puncta (Fig. 10A and B). Knockdown any of the three genes reduced the level of LC3-II, a form of LC3 modified with phosphatidylethanolamine at C-terminus (Fig. 10C). We also found that the expression level of p62/SQSTM1, a protein degraded through autophagy (Mizushima 2007), is

higher in ULK1, ULK2 or Atg5-silenced adipocytes compared to that in control cells (Fig. 10C). EM images of autophagosomes confirmed a significant reduction in the number of autophagosomes in ULK1, ULK2 or Atg5-silenced adipocytes compared to control cells (Fig. 11A and B). Combined, these results suggest that ULK1, ULK2 and Atg5 are important for basal autophagy in adipocytes.

Rapamycin, a potent inducer of autophagy, increased the LC3-positive puncta formation in control adipocytes (Fig. 10A and B). The puncta formation was significantly suppressed by knockdown of ULK1, ULK2 or Atg5. Rapamycin increased the level of LC3-II in ULK1, ULK2, or Atg5-silenced adipocytes to a much lesser extent than in control cells. Consistent with the marginal change of LC3-II level, rapamycin barely reduced p62 level in the cells where the autophagy genes were knocked down (Fig. 10C). The knockdown effect on LC3 processing was highest with Atg5 knockdown (Fig. 10C). Consistent with this finding, recent reports showed that knockdown of either ULK1 or ULK2 had only a moderate effect on LC3 processing in other cell types (Hosokawa N 2009; Jung CH 2009). This might be because ULK1 and ULK2 could compensate each other when either gene was knocked down. Alternatively, the stronger effect by Atg5 knockdown might be due to the critical function of Atg5 as part of the LC3 conjugation machinery (Mizushima N 2001; Tanida I 2004). Combined, these results suggest that ULK1, ULK2 and Atg5 are important for both basal and rapamycin-induced autophagy in 3T3-L1 adipocytes.

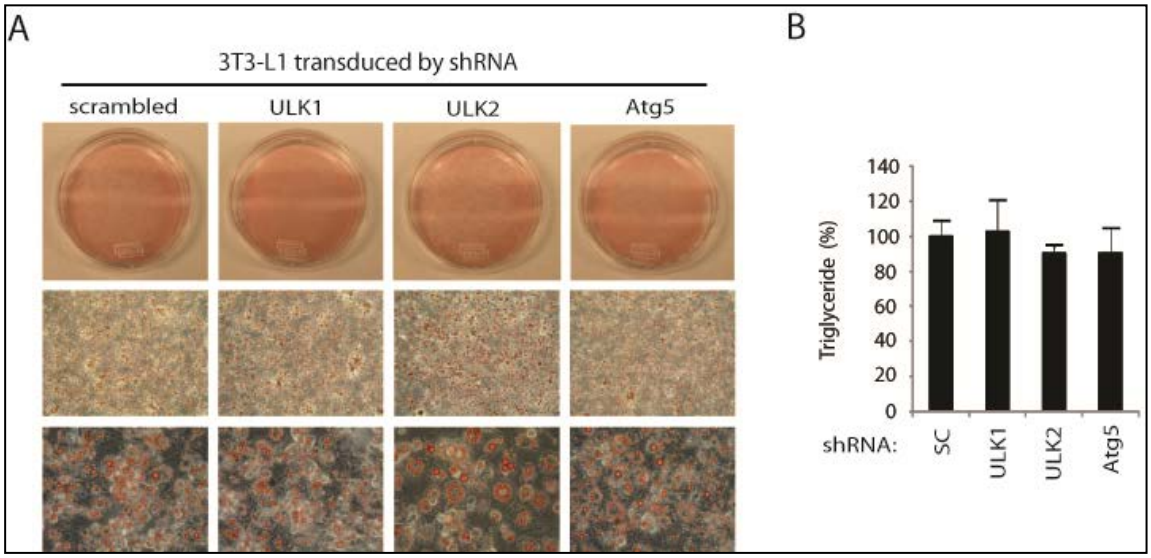

Figure 9. 3T3-L1 predipocytes stably transduced by shRNAs were fully differentiated and used for metabolic assays. (A) ULK1, ULK2 or Atg5-silenced L1 cells and scrambled shRNA-transduced L1 cells were differentiated as described previously (Curtis JM 2010) in the presence of 5 μM troglitazone. (B) Quantitative measurement of intracellular triglyceride using Oil Red O. Values are mean ± std. from three independent experiments. Detailed procedures are described in Materials and Methods section.

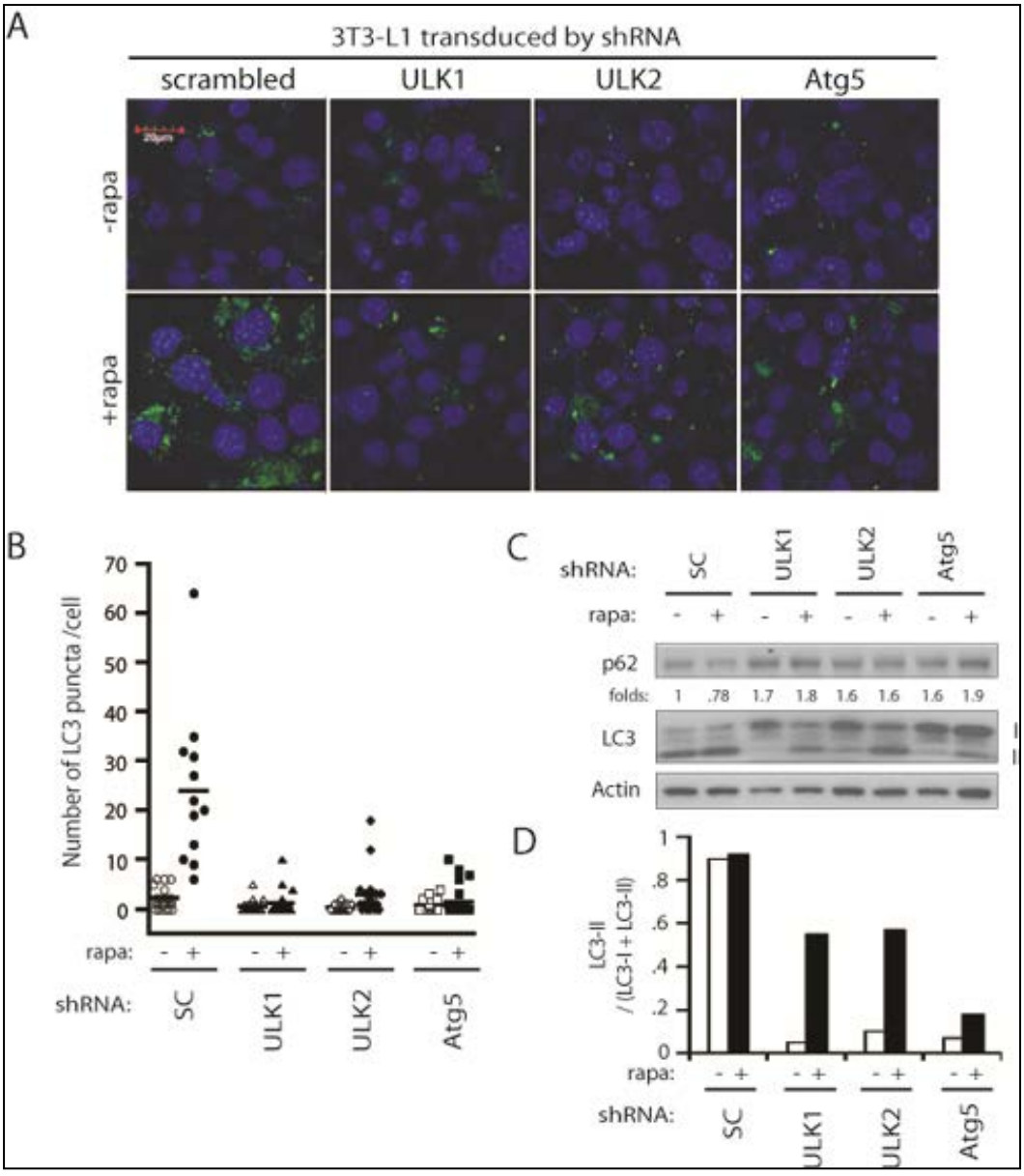
A
3T3-L1 transduced by shRNA
scrambled
ULK1
ULK2
Atg5
-rapa
+rapa
B
Number of LC3 puncta /cell
70
60
50
40
30
20
10
0
rapa: - + - + - + - +
shRNA: SC ULK1 ULK2 Atg5
C
shRNA: SC ULK1 ULK2 Atg5
rapa: - + - + - + - +
p62
folds: 1 .78 1.7 1.8 1.6 1.6 1.6 1.9
LC3
Actin
D
LC3-II / (LC3-I + LC3-II)
1
.8
.6
.4
.2
0
rapa: - + - + - + - +
shRNA: SC ULK1 ULK2 Atg5

Figure 10. ULK1, ULK2 and Atg5 are important for autophagy in adipocytes. (A) Knockdown of ULK1, ULK2 or Atg5 inhibits the formation of autophagosome in adipocytes. 3T3-L1 adipocytes stably transduced by lentiviral shRNA were treated with rapamycin or DMSO for 5 h in the presence of lysosomal inhibitors (pepstatin A and E-64). LC3 puncta were monitored by immunostaining endogenous LC3 using anti-LC3 antibody (green). Nucleus was stained by DAPI (blue). Detailed procedures are described in Materials and Methods section. (B) The number of LC3 puncta was counted per each cell and quantitatively analyzed. The horizontal bar represents mean value. (C) Knockdown of ULK1, ULK2, or Atg5 suppressed the conversion of LC3-I to LC3-II and the autophagic degradation of p62. LC3 and p62 in cell lysates obtained from (A) were analyzed by Western blotting. (D) Quantitative analysis of LC3-II level relative to LC3-I level. The y-axis represents the ratio of LC3-II level versus the levels of LC3-I and LC3-II combined.

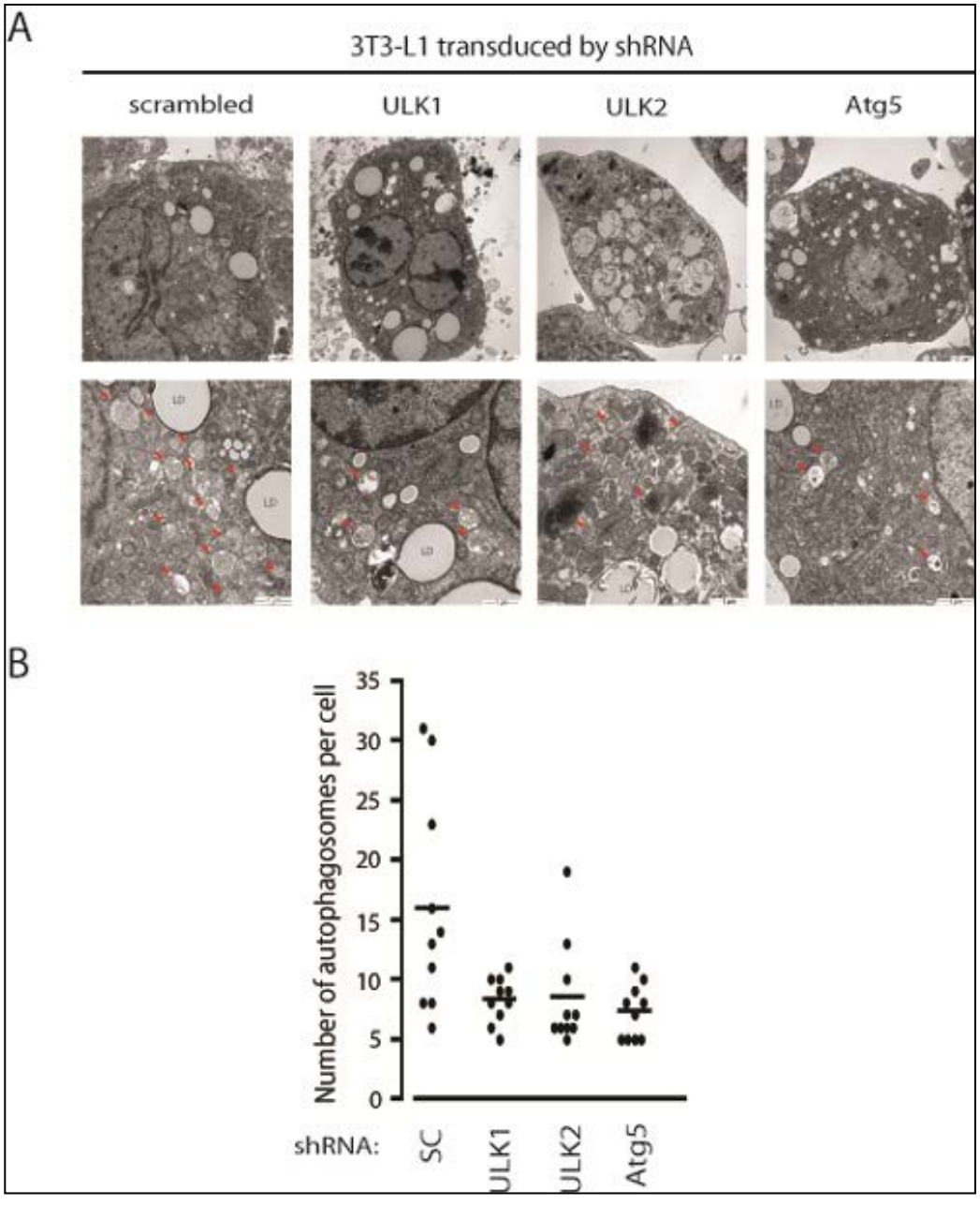
A
3T3-L1 transduced by shRNA
scrambled
ULK1
ULK2
Atg5
B
Number of autophagosomes per cell
35
30
25
20
15
10
5
0
shRNA:
SC
ULK1
ULK2
Atg5

Figure 11. EM analysis of autophagosomes reveals autophagy activity in 3T3-L1 adipocytes. (A) EM image of 3T3-L1 adipocytes (day 8 after induction of differentiation). Red arrows indicate autophagosomes. LD, lipid droplets. Detailed procedures are described in Materials and Methods section. (B) Quantitative analysis of the number of autophagosomes per each cell from EM images. The horizontal bar represents mean value.

2.3. Conclusion

Through the analysis of autophagy activity in adipose tissue, my study revealed that autophagy activity in adipose tissue was increased from mice fed with high fat diet. The increase in the activity of adipocyte autophagy could be due to a cellular protective mechanism against the metabolic stress, rather than due to any causative effect of autophagy on the development of such disease states. This effect is consistent with recent reports showing an increase in the activity of adipocyte autophagy in diabetic and obese states (Kovsan J 2011; Ost A 2010; Zhang Y 2009; Zhou L 2009). This protective function of autophagy might be important especially when adipocytes are under metabolic stress. Another key finding is that ULK1 and ULK2 are important for basal and rapamycin-induced autophagy in adipocytes. These results provided the basis on which my thesis studies have been developed as described in the following chapters.

CHAPTER 3 : Distinct functions of the ULK1 and ULK2 in adipocyte metabolism

Introduction : Knowing that ULK1 and ULK2 are important for adipocyte autophagy, the aim of my study in this chapter was to analyze the functions of ULK1 and ULK2 in the regulation of adipocyte metabolism. This chapter is focused on the distinct functions of ULK1 and ULK2 in the regulation of adipogenesis and adipocyte metabolism, whereas the following chapter is focused on the shared functions of the kinases. I performed multiple metabolic assays to assess the effects of ULK1 and ULK2 knockdown on adipogenesis, lipolysis, glucose uptake, fatty acid oxidation, fatty acid synthesis and mitochondrial functions. Key findings with regard to distinct effects of ULK1 and ULK2 on the metabolic parameters are described in the following sections.

3.1. ULK1 and ULK2 have opposing effects on adipogenesis.

Knowing that ULK1 and ULK2 are important for adipocyte autophagy, we inquired whether they are important for adipogenesis. Because previous studies have shown that Atg5 and Atg7 are important for adipogenesis (Baerga R 2009; Singh R 2009; Zhang Y 2009), we anticipated that knockdown of ULK1 or ULK2 would affect adipogenesis. In the experiment above, we treated cells with TZD to achieve full differentiation. To assess the extent of differentiation, we excluded TZD in our differentiation protocol following the procedure described previously (Student AK 1980; Lobo S 2007). The GFP-shRNA transduced 3T3-L1 cells started to show lipid accumulation at day 4 after induction of differentiation. Compared to the control cells, ULK1-silenced cells initiated the lipid accumulation earlier during the days 2 – 3 (Fig. 12). By contrast, ULK2-silenced cells showed a delay in lipid accumulation compared to control cells (Fig. 12). At day 8, we quantitatively analyzed the extent of differentiation by analyzing the lipid droplet contents. ULK1-silenced 3T3-L1 cells had a higher level of lipid droplet contents with a 11 % increase than GFP shRNA-transduced cells (Fig. 13A and B). To exclude any off-target effect by shRNA, we confirmed the result by using other ULK1 shRNA with a different target site (Fig. 14). By contrast, ULK2-silenced L1 cells had a lower level of lipid droplet contents with a 24 % reduction compared to control cells (Fig. 13A and B). To clarify whether the effects of ULK1 and ULK2 knockdown on adipogenesis are related to autophagy, we analyzed the effects of knockdown of Atg5 on adipogenesis. Atg5 knockdown decreased lipid droplet content by 12 %. This result

suggests that ULK2 effects on adipogenesis might be related to Atg5-mediated autophagy. This result is consistent with the result from other groups using Atg5 and Atg7-silenced adipocytes (Singh R 2009).

We also analyzed differentiation marker proteins in the stable cells. Peroxisome proliferator-activated receptor-γ (PPAR-γ) and CCAAT/enhancer binding protein-α (CEBP-α) are two key transcription factors involved in adipogenesis (Tontonoz P 2008). We found that PPAR-γ is greatly increased in ULK1 silenced cells (Fig. 13C and 14C). Although the level of PPAR-γ was not increased in Atg5-silenced adipocytes, the level of CEBP-α p42 was increased (Fig. 13C). In contrast, both PPAR-γ and CEBP-α were significantly reduced in ULK2 silenced cells, consistent with the lowest level of differentiation with these cells. Sterol regulatory element-binding protein-1 (SREBP-1), the key transcription factor involved in lipid metabolism (Tontonoz P 2008), was not significantly changed by any of the knockdowns (Fig. 13C). We found that ULK2 knockdown increases the level of ULK1, suggesting that there is likely a compensatory mechanism existing between ULK1 and ULK2 (Fig. 13C). Thus, it is possible that the inhibitory effect of ULK2 knockdown on adipogenesis is related to the increase in ULK1 level.

Interestingly, when both ULK1 and ULK2 were knocked down, the differentiation was suppressed in a similar extent as the knockdown of ULK2 alone (Fig. 15). This result suggests that the inhibitory effects of ULK2 knockdown on adipogenesis are unlikely

due to the increase of ULK1 level but rather due to inhibition of ULK2-dependent steps crucial for adipogenesis. Given the similar effects of ULK2 and Atg5 on adipocyte differentiation, ULK2 rather than ULK1 is likely more closely linked to Atg5 in the regulation of adipocyte differentiation.

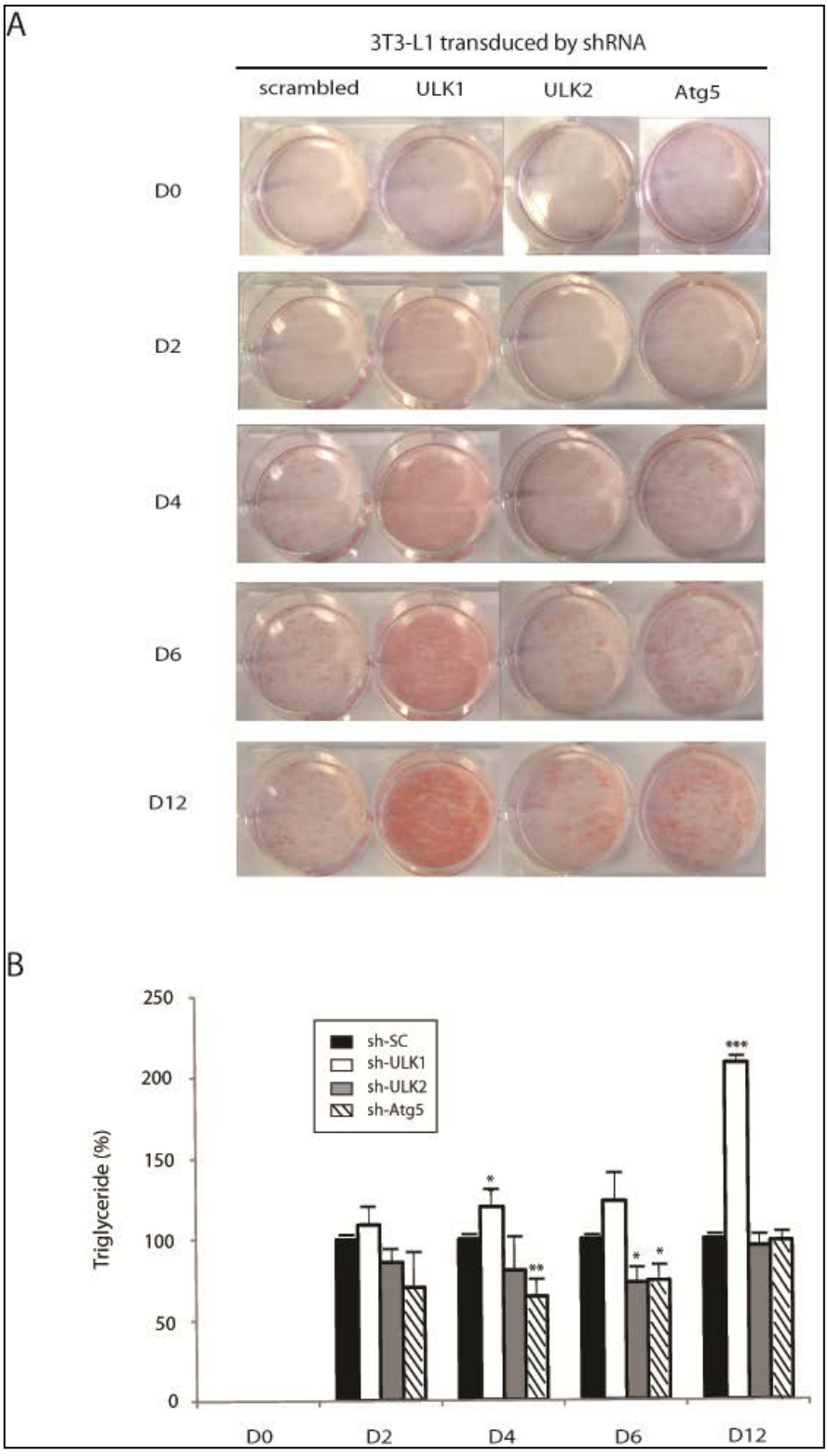
A
3T3-L1 transduced by shRNA
scrambled
ULK1
ULK2
Atg5
D0
D2
D4
D6
D12
B
Triglyceride (%)
250
200
150
100
50
0
sh-SC
sh-ULK1
sh-ULK2
sh-Atg5
*
**
*
*
***
D0
D2
D4
D6
D12

Figure 12. Adipocyte differentiation without troglitazone in multiple days. (A) ULK1, ULK2 or Atg5-silenced L1 cells and scrambled shRNA-transduced L1 cells were differentiated with insulin, methylisobutylxanthine, and dexamethasone, but without troglitazone. Detailed procedures are described in Materials and Methods section. (B) Measurement of intracellular triglyceride in multiple days. Values are mean ± std. *, $p < 0.05$; **, $p < 0.01$; ***, $p < 0.001$

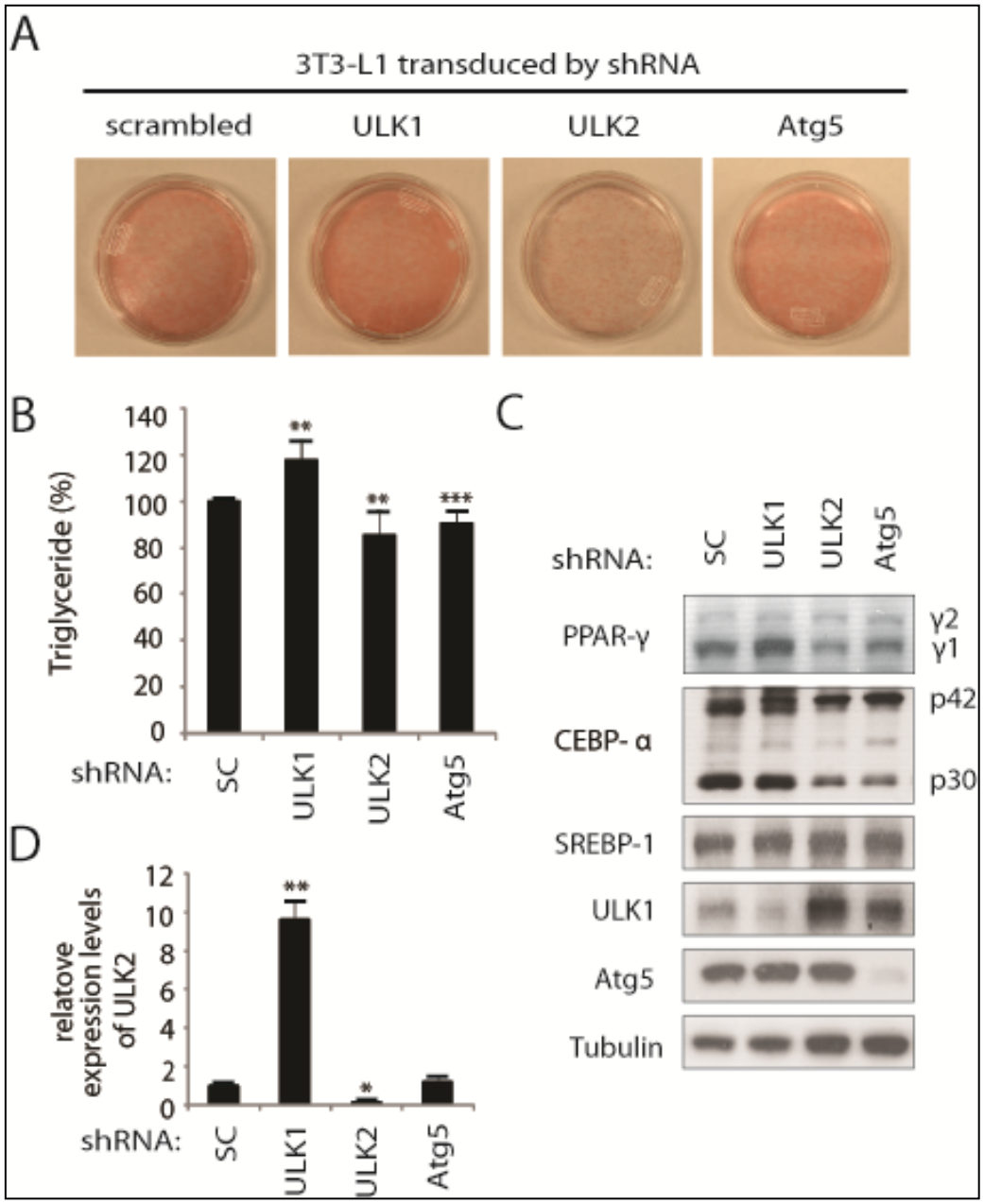
A
3T3-L1 transduced by shRNA
scrambled
ULK1
ULK2
Atg5
B
Triglyceride (%)
140
120
100
80
60
40
20
0
**
**
***
shRNA:
SC
ULK1
ULK2
Atg5
C
shRNA:
SC
ULK1
ULK2
Atg5
PPAR-γ
γ2
γ1
CEBP- α
p42
p30
SREBP-1
ULK1
Atg5
Tubulin
D
relatove expression levels of ULK2
12
10
8
6
4
2
0
**
*
shRNA:
SC
ULK1
ULK2
Atg5

Figure 13. ULK1 and ULK2 have opposite effects on adipogenesis. (A) 3T3-L1 cells stably transduced by shRNA were differentiated in the absence of troglitazone. Cells were stained by Oil red O at day 8 after differentiation was induced. (B) Quantitative analysis of 3T3-L1 cell differentiation in the absence of troglitazone. Intracellular triglyceride content was analyzed by extracting Oil Red O from cells with use of isopropanol and measuring the optical density of the extracted Oil Red O at wavelength of 490 nm. (C) Western blot analysis of protein expression in adipocytes. Cell lysate was obtained from cells differentiated in the absence of troglitazone. (D) Knockdown of ULK2 was confirmed by RT-PCR due to lack of antibody available to detect mouse ULK2. About 85% of knockdown was confirmed for mouse ULK2 (NM_013881) by RT-PCR. Values are mean ± std. *, $p < 0.05$; **, $p < 0.01$; ***, $p < 0.001$. Detailed procedures are described in Materials and Methods section.

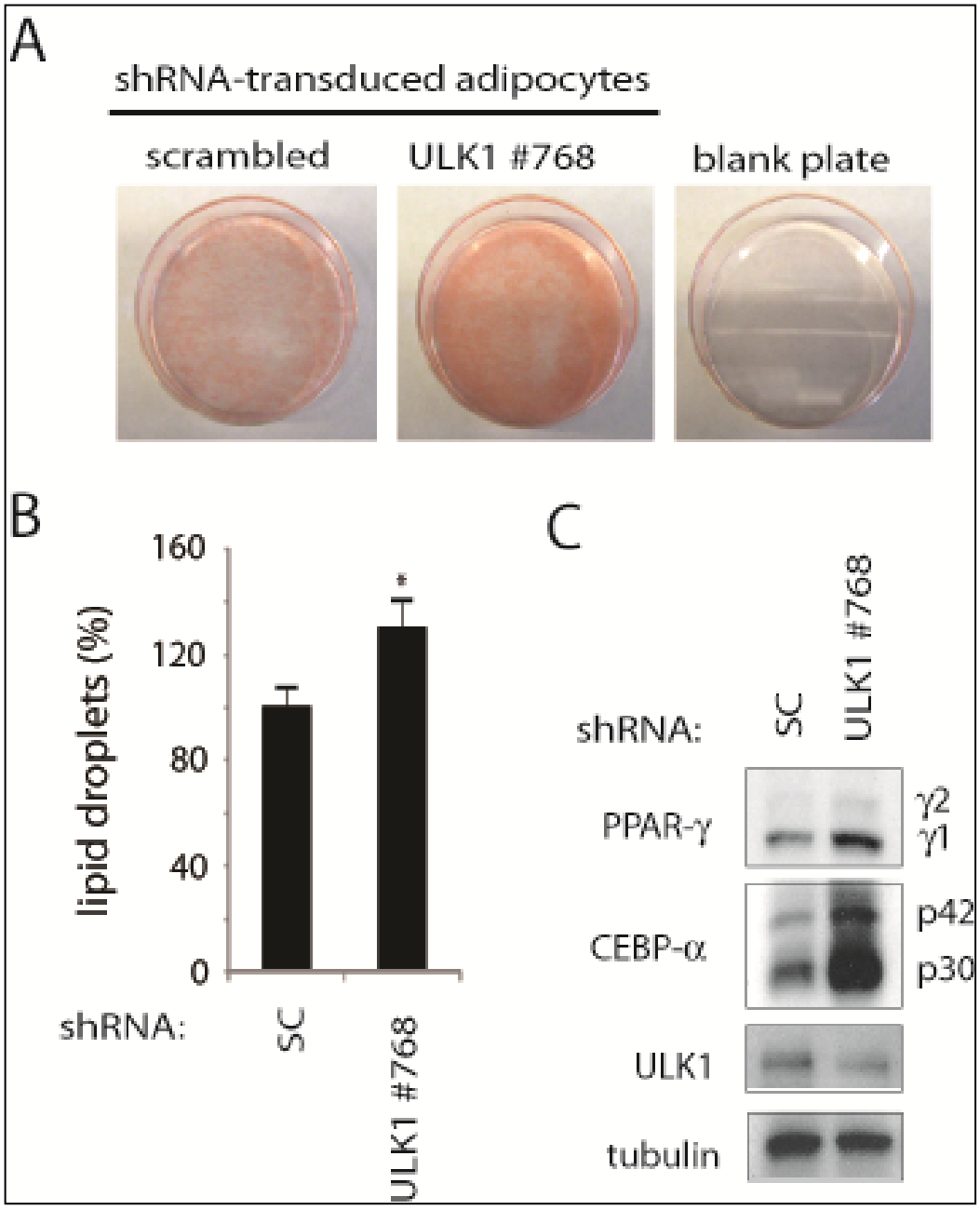
A
shRNA-transduced adipocytes
scrambled
ULK1 #768
blank plate
B
lipid droplets (%)
160
120
80
40
0
*
shRNA:
SC
ULK1 #768
C
shRNA:
SC
ULK1 #768
PPAR-γ
γ2
γ1
CEBP-α
p42
p30
ULK1
tubulin

Figure 14. Effect of ULK1 inhibition using different sh-RNA sequence (#768) on adipocyte differentiation. Adipocyte differentiation was increased with the reduced lipid droplet size in ULK1-knocked down adipocytes when using different sh-RNA sequence (#768, Table S2) (A) Autophagy gene silenced cells are differentiated. Lipid droplet of differentiated cells was stained using Oil red O. (B) Intracellular Triglyceride was measured. After extracting Oil Red O from cells with isopropanol, optical density (OD) was measured at a wavelength of 490 nm. Values are mean ± std. *, $p < 0.05$. (C) Protein expression levels of adipose differentiation indicators, PPAR-γ and CEBPα were shown by western blotting in scrambled, ULK1 (#768) silenced cells after lysed in RIPA buffer. Silencing of targeted ULK1 gene by #768 sh-RNA sequence was confirmed by western blotting in ULK1 silenced cells.

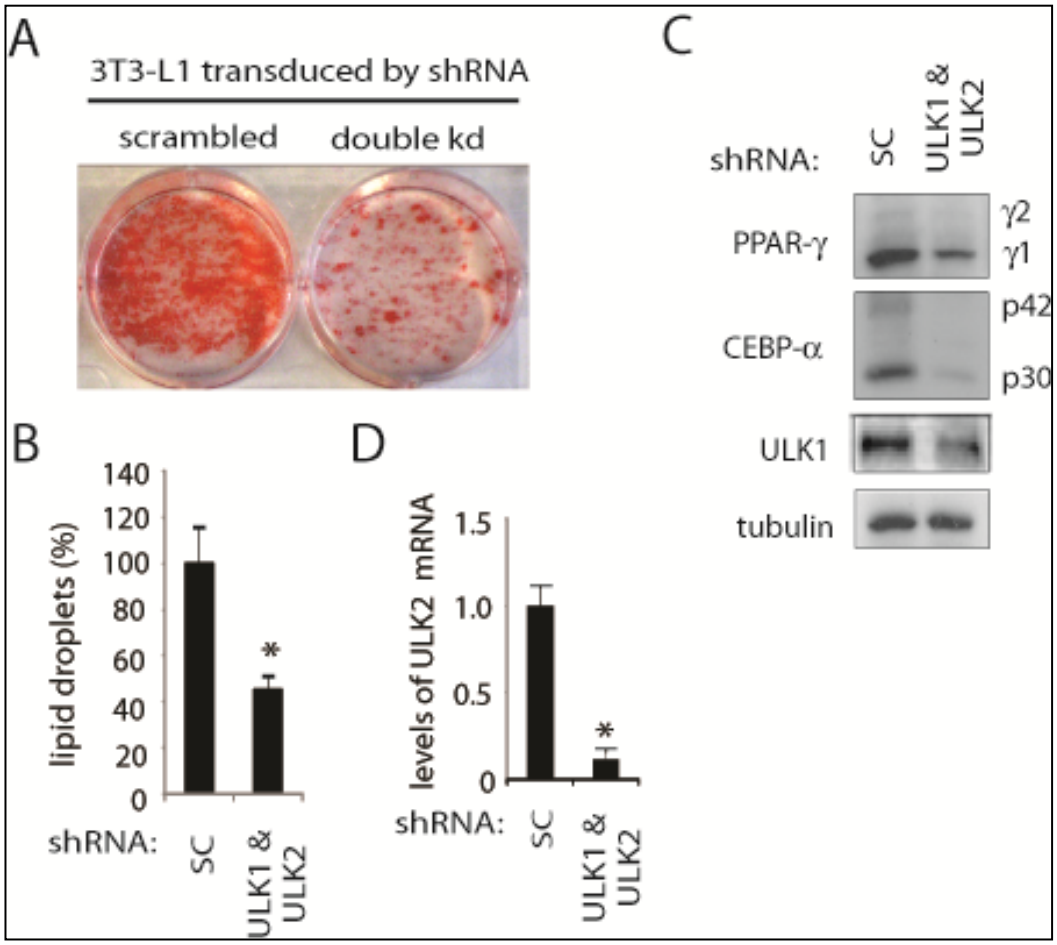
A
3T3-L1 transduced by shRNA
scrambled
double kd
B
lipid droplets (%)
140
120
100
80
60
40
20
0
*
shRNA:
SC
ULK1 & ULK2
C
shRNA:
SC
ULK1 & ULK2
PPAR-γ
γ2
γ1
CEBP-α
p42
p30
ULK1
tubulin
D
levels of ULK2 mRNA
1.5
1.0
0.5
0
*
shRNA:
SC
ULK1 & ULK2

Figure 15. Effect of ULK1 and ULK2 double knockdown on adipocyte differentiation. Adipocyte differentiation was decreased in ULK1 and ULK2 double-knocked down adipocytes (A) Both ULK1 and ULK2 silenced cells are differentiated. Lipid droplet of differentiated cells was stained using Oil red O. (B) Intracellular Triglyceride was measured. After extracting Oil Red O from cells with isopropanol, optical density (OD) was measured at a wavelength of 490 nm. (C) Protein expression levels of adipose differentiation indicators, PPAR-γ, CEBP-α, and SREBP-1 was shown by western blotting in scrambled, both ULK1 and ULK2 silenced cells after lysed in RIPA buffer. Silencing of targeted ULK1 gene was confirmed by western blotting in ULK1/ULK2 double-knocked down adipocytes (D) Silencing of targeted ULK2 gene was confirmed by RT-PCR in ULK2 silenced cells. Values are mean ± std. *, $p < 0.05$

3.2. ULK1 plays critical roles in lipolysis and fatty acid oxidation.

Noting the difference in adipogenesis in ULK1 or ULK2 knockdown adipocytes, we asked whether utilization of lipid as energy source has been altered in those cells (Curtis JM 2010). Supporting this notion, the gene expression levels of ACC1, ACC2, and FASN involved in fatty acid synthesis were dramatically increased in ULK1 silenced cells. In contrast, the mRNA levels of ACC2 and FASN in ULK2 silenced cells and the mRNA level of ACC2 in Atg5 silenced cells were reduced compared to control cells (Fig. 16A). Increased gene expression of fatty acid synthesis in ULK1 silenced cells and decreased level in ULK2 or Atg5 silenced cells correlates with the increased amount of fat depots in ULK1 silenced cells and decreased amount of fat depots in ULK2 or Atg5 silenced cells (Fig. 13)

Knowing that there were changes in lipid metabolism, we wondered whether fatty acid oxidation may also be affected. To assess mitochondrial beta oxidation, the conversion of radio-labeled oleate to CO_2 was assayed (Koves TR 2005). ULK1-silenced adipocytes exhibited 8% reduction in fatty acid oxidation of [1-^{14}C]-oleate as determined by the production of ^{14}C-labeled CO_2 whereas ULK2 or Atg5 knockdown adipocytes had 25% and 38% increase in fatty acid oxidation, respectively (Fig. 16B). These results suggest that breakdown of fat depots and subsequent oxidation of fat as energy source is significantly enhanced by ULK2 knockdown or Atg5 knockdown whereas accumulation of fat depot are dominant over breakdown in ULK1 knockdown. However, when we

analyzed lipolysis of non-esterified fatty acids from ULK1 and ULK2 silenced adipocytes, the silencing of ULK1 or ULK2 led to an ~20% decrease in basal lipolysis (Fig. 16C). By contrast, cyclic AMP (cAMP)-dependent lipolysis was not significantly affected by knockdown of ULK1, ULK2 or Atg5 (Fig. 16D). A possible role for ULK1, ULK2 and Atg5 in lipolysis might be related to the macroautophagic degradation of lipid droplets as was shown in hepatocytes (Singh R 2009). Due to a high content of lipid droplets in adipocytes, we could not detect small lipid droplets. However, we could observe that some small lipid droplets colocalize with autophagosome in adipocytes (Fig. 17). Thus, the macroautophagic degradation of lipid droplets might be a possible process occurring in adipocytes. The similar inhibitory effects on lipolysis between ULK1, ULK2 and Atg5 indicate that lipolysis may not be responsible for the different effects on differentiation.

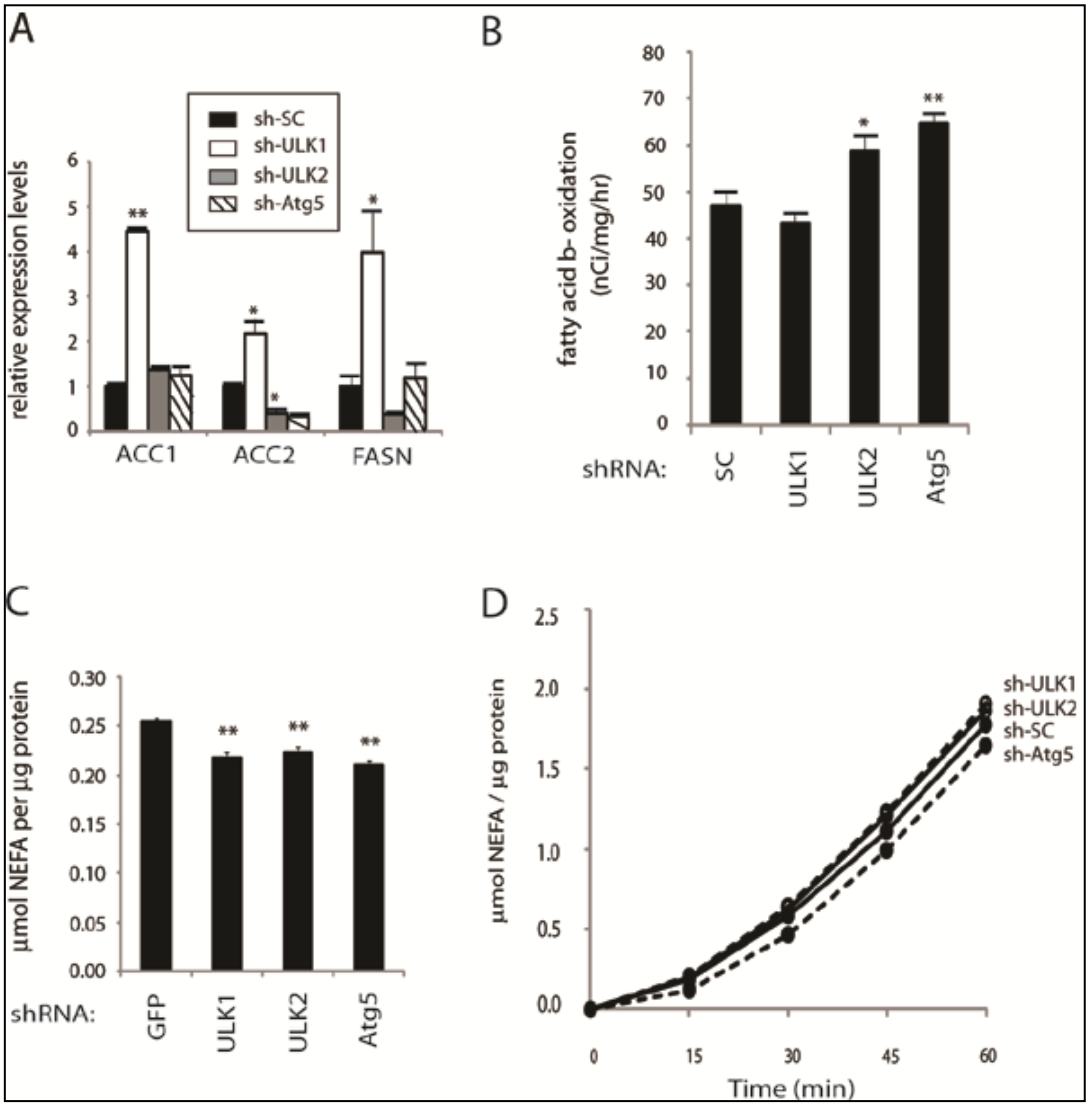
A
relative expression levels
sh-SC
sh-ULK1
sh-ULK2
sh-Atg5
ACC1
ACC2
FASN
B
fatty acid b- oxidation (nCi/mg/hr)
shRNA:
SC
ULK1
ULK2
Atg5
C
µmol NEFA per µg protein
shRNA:
GFP
ULK1
ULK2
Atg5
D
µmol NEFA / µg protein
sh-ULK1
sh-ULK2
sh-SC
sh-Atg5
Time (min)

Figure 16. ULK1 and ULK2 differently regulate fatty acid synthesis and oxidation, whereas both kinases are important for lipolysis. (A) Expression of ACC1, ACC2, and FASN involved in fatty acid metabolism was quantitatively analyzed by RT-PCR. Values are mean ± std. *, $p < 0.05$; **, $p < 0.01$. (B) ULK1 enhances β-oxidation, whereas ULK2 reduces β-oxidation. β-oxidation was assayed using [^{14}C]-oleic acid. (C) Knockdown of ULK1, ULK2 or Atg5 reduces basal lipolysis. 3T3-L1 adipocytes transduced by shRNA were incubated at 37ºC in KRH supplemented with 2% fatty acid-free BSA and 5 mM glucose. Media was collected after 60 minutes and the non-esterified fatty acids determined using NEFA-HR assay kit (D) Forskolin-stimulated lipolysis was not significantly affected by knockdown of ULK1, ULK2 or Atg5. The level of fatty acids in the medium was analyzed during the indicated period of time by use of NEFA-HR assay kit. Values are mean ± std from three independent experiments. *, $p < 0.05$; **, $p < 0.01$. Detailed procedures are described in Materials and Methods section.

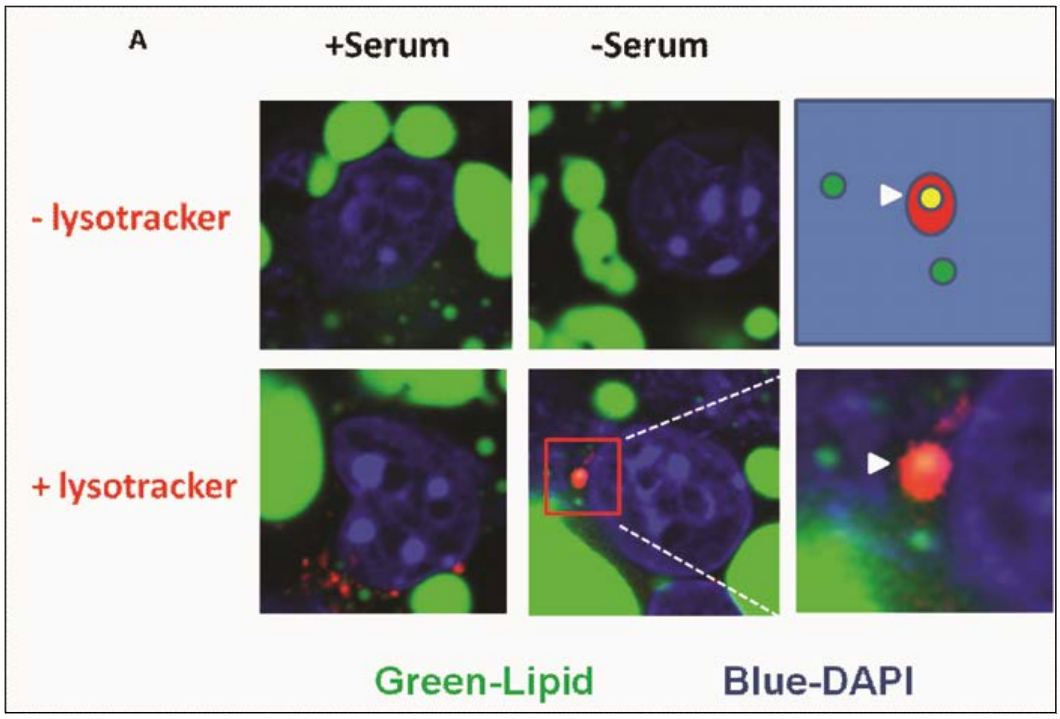

Figure 17. Evidence of autophagic clearance of lipid droplet in adipocytes. Fully-differentiated 3T3-L1 cells were cultured in the presence or absence of serum for 2 hours. Serum starvation is known to induce macroautophagy. Lysosomes were stained using 50 nM lysotracker (Invitrogen) for 30 min, and visualized by fluorescence microscopy. Lipid droplets were stained by lipid-specific dye, BODIPY (Invitrogen). Detailed procedures are described in Materials and Methods section.

3.3. Conclusion

My study revealed that ULK1 has distinct functions from ULK2 and Atg5 in the regulation of adipogenesis and lipid metabolism in adipocytes. ULK1 knockdown enhanced adipogenesis in 3T3-L1 cells, which has not been observed with other autophagy-related proteins. This result suggests that autophagy activity does not necessarily correlate with the extent of adipogenesis, opposing the previously shown function of adipocyte autophagy (Baerga R 2009; Singh R 2009; Singh R 2009; Zhang Y 2009). I also found that ULK1 and ULK2 have different effects on the expression of genes involved in fatty acid synthesis. The up-regulation of the genes involved in fatty acid synthesis by ULK1 knockdown could be at least in part due to the up-regulation of PPAR-γ (Li AC 2004), defining a novel function of ULK1 in the PPAR-γ pathway. We found that ULK1 and ULK2 have opposing effects on fatty acid oxidation and insulin-stimulated glucose uptake. These changes are consistent with the opposing effects of ULK1 and ULK2 on adipogenesis. I found that the extent of adipogenesis correlates well with the level of ULK2 rather than ULK1, and that ULK2 has a dominant effect over ULK1 in the regulation of adipogenesis. It is also noteworthy that knockdown of ULK2 dramatically enhanced the expression level of ULK1 while still inhibiting autophagy. These results support the important function of ULK2 as a key factor required for autophagy and adipogenesis in adipocytes. This function of ULK2 does not appear to be replaced by ULK1.

CHAPTER 4 : Shared functions of ULK1 and ULK2 in adipocyte metabolism

Introduction : The previous chapter described that ULK1 and ULK2 have distinct functions in adipogenesis and lipid metabolism. This chapter is focused on the shared functions of ULK1 and ULK2 in the regulation of adipocyte metabolism. I performed multiple metabolic assays to assess the effects of ULK1 and ULK2 knockdown on insulin/Akt/mTORC1 signaling activity, glucose metabolism, mitochondria functions, and oxidative stress response. I found that both ULK1 and ULK2 are important for the mitochondrial function and oxidative stress response of adipocytes. Key findings with regard to the shared effects of ULK1 and ULK2 on the metabolic parameters are described in the following sections.

4.1. ULK1 and ULK2 negatively regulate mTORC1 signaling in adipocytes.

Knowing that the insulin/mTORC1 signaling pathway is important for adipogenesis (Zhang HH 2009), we wondered if the pathway is affected differently by ULK1 or ULK2 knockdown. The fully differentiated shRNA-transduced adipocytes were treated with insulin and the phosphorylation states and the expression levels of Akt and S6K1 were analyzed. We found that knockdown of ULK1 or ULK2 enhanced the phosphorylation of S6K1 at Thr389 to a greater extent than control cells (Fig. 18A and B). These results are consistent with previous reports showing that ULK1 and ULK2 have negative effects on S6K1 phosphorylation in 293T, HeLa, and MEFs. ULK1 homolog Atg1 has negative effects on mTORC1 pathway in *Drosophila* (Lee SB 2007; Scott RC 2007). Although previous studies revealed that ULK1 has a direct inhibitory effect on mTORC1 (Dunlop EA 2011; Jung CH 2011), S6K1 phosphorylation was also increased by knocking down Atg5 (Fig. 18B). Therefore, there may exist a mechanism, distinct from the previously-proposed one, through which autophagy regulates mTORC1 (Dunlop EA 2011; Jung CH 2011). On the other hand, knockdown of either ULK1 or ULK2 did not alter the phosphorylation status of Akt at S473. Similarly, Atg5 knockdown enhanced S6K1 phosphorylation to a level similar to that observed with ULK2 knockdown and did not have an effect on Akt phosphorylation (Fig. 18A and B). This suggests that the increase of S6K1 phosphorylation may occur in a manner independent of Akt. Interestingly, knockdown of ULK1, but not knockdown of neither ULK2 nor Atg5, increased the levels of IRβ and IRS-1 (Fig. 18A and B). Thus, it is

possible that the up-regulation of IRβ and IRS-1 levels and subsequent activation of growth factor signaling in ULK1-silenced cells might be involved in the up-regulation of adipogenesis, although this pathway seems not to affect Akt activation.

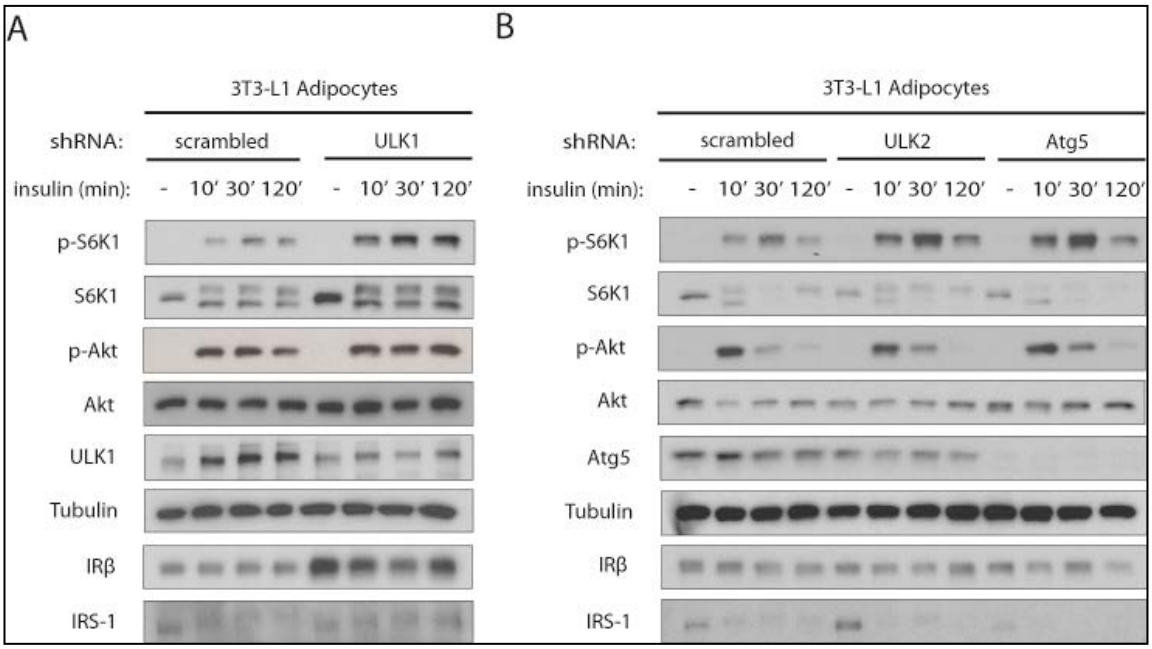

Figure 18. ULK1 and ULK2 negatively regulate the mTORC1 signaling in adipocytes. (A) Knockdown of ULK1 enhances mTORC1 signaling. 3T3-L1 adipocytes transduced by shRNA were starved of serum overnight and treated with insulin for the indicated period of time. Cell extract was obtained and the expression levels and phosphorylation states of the indicated proteins were analyzed by Western blot. (B) Knockdown of ULK2 or Atg5 enhances mTORC1 signaling in adipocytes.

4.2. ULK1 and ULK2 negatively regulate glucose uptake and glycolysis.

Knowing that ULK1 and ULK2 regulate mTOR signaling, we inquired whether ULK1 and ULK2 would regulate other metabolic parameters related to adipocyte metabolism. One of the important metabolic activities in adipocytes is glucose metabolism (Bittner CX 2010). To investigate whether glucose transport is affected by ULK1 and ULK2, we assayed uptake of 2-deoxyglucose (2-DG), the non-hydrolyzable analog of glucose, into adipocytes. 2-DG uptake rate was increased by 28% in ULK1 knockdown and 23% in ULK2 knockdown compared to control cells (Fig. 19A). The level of glucose transporter (GLUT) 1 responsible for basal glucose uptake was also higher in ULK1 or ULK2 knock downed cells (Fig. 19D). Knowing the involvement of ULK1, ULK2 and Atg5 in glucose transport, we assayed glycolytic rate by measuring H^+ in medium. We found that knockdown of ULK1, ULK2 or Atg5 increased glycolysis rate by 1.7, 1.4 and 1.8 folds compared to control cells, respectively (Fig. 19C). Thus, the autophagy proteins likely affect the basal glucose uptake. Up-regulation of GLUT1 through unknown mechanism might be responsible at least in part for the increase in the basal glucose uptake rate.

We also analyzed glucose uptake rate in response to insulin. ULK1 knockdown enhanced glucose uptake rate by about 1.4 fold (Fig. 19B). On the other hand, glucose uptake rate in ULK2- and Atg5-silenced adipocytes was about 85% relative to that in control cells. The increase by ULK1 knockdown was accompanied with an increase in

the expression level of GLUT4, the glucose transport responsible for insulin-stimulated glucose uptake (Fig. 19D). Such an increase in GLUT4 level was not observed with ULK2- and Atg5-silenced adipocytes. PPAR-γ is known to up-regulate GLUT4 expression in adipocytes (Hamm JK 1999; Liao W 2007). PPAR-γ that was also up-regulated in ULK1-silenced cells (Fig. 13C and 14C). Thus, the up-regulation of GLUT4 by ULK1 knockdown could be due to PPAR-γ.

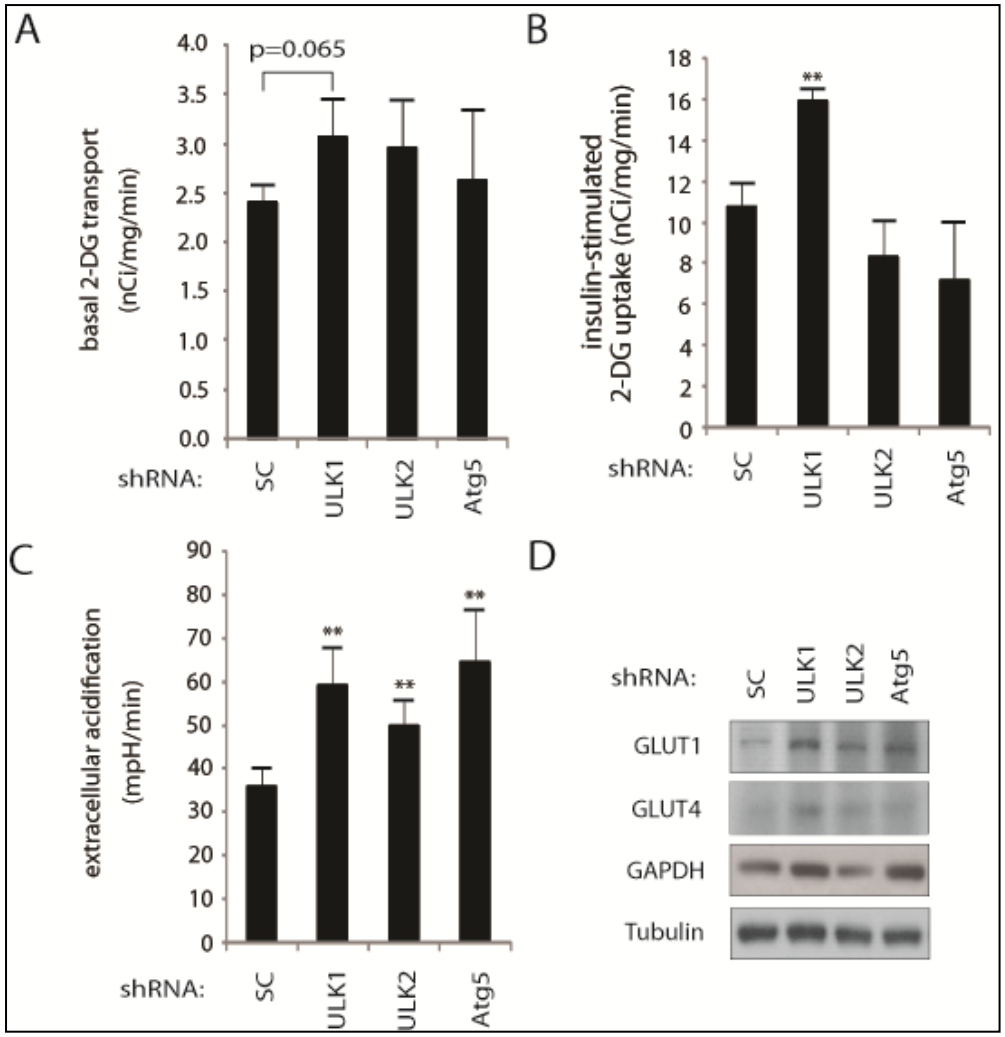
A
basal 2-DG transport (nCi/mg/min)
p=0.065
4.0
3.5
3.0
2.5
2.0
1.5
1.0
0.5
0.0
shRNA:
SC
ULK1
ULK2
Atg5
B
insulin-stimulated 2-DG uptake (nCi/mg/min)
**
18
16
14
12
10
8
6
4
2
0
shRNA:
SC
ULK1
ULK2
Atg5
C
extracellular acidification (mpH/min)
**
**
**
90
80
70
60
50
40
30
20
10
0
shRNA:
SC
ULK1
ULK2
Atg5
D
shRNA:
SC
ULK1
ULK2
Atg5
GLUT1
GLUT4
GAPDH
Tubulin

Figure 19. ULK1, ULK2 and Atg5 negatively regulate glycolysis. (A) Knockdown of ULK1, ULK2, and Atg5 enhanced basal glucose uptake. Adipocytes were incubated in the presence of [^{3}H]-2-deoxyglucose for 5 min. Cells were then incubated with [^{3}H]-2-deoxyglucose for 5 min. Cells were harvested and the amount of [^{3}H]-2-deoxyglucose in harvested cells was assayed by using a scintillation counter. The amount of [^{3}H]-2-deoxyglucose in harvested cells was assayed (n = 3). (B) Knockdown of ULK1 enhances insulin-stimulated glucose uptake rate, whereas knockdown of ULK2 or Atg5 suppressed it. Adipocytes were starved of serum overnight then stimulated with insulin for 60 min. (C) Knockdown of ULK1, ULK2, and Atg5 increased extracellular acidification. The level of extracellular acidification was measured using XF24 extracellular flux analyzer. Data are presented as percentage relative to scrambled shRNA-transduced adipocytes. (D) The expression levels of GLUT1, GLUT4 glucose transporter, and GAPDH were analyzed by Western blotting. Values are mean ± std. *, $p < 0.05$; **, $p < 0.01$. Detailed procedures are described in Materials and Methods section.

4.3. ULK1 or ULK2 are important for mitochondria respiration in adipocytes.

Knowing that ULK1 and ULK2 have effects on fatty acid oxidation, we inquired whether the kinases regulate the function of mitochondria. To determine the effects of ULK1 and ULK2 knockdown on mitochondrial function, we examined a variety of metabolic parameters linked to mitochondria (Curtis JM 2010). First, we evaluated markers of mitochondrial biogenesis at protein, mRNA and DNA levels. The expression of the key transcription factors Tfam, eNOS, and PGC-1α involved in mitochondrial biogenesis were greatly increased by ULK1 and ULK2 knockdown (Fig. 20A). Consistent with the increased expression of the genes regulating mitochondria biogenesis, the abundance of COX II gene was significantly increased by ULK1, ULK2 or Atg5 knockdown (Fig. 20B). These results indicate that the accumulation of damaged mitochondria which are not cleared by autophagy was more severe in ULK1 knockdown compared to ULK2 or Atg5 knockdown.

Interestingly, among the antioxidant response genes, the expression levels of GSTA4 and NQO-1 were increased in ULK2- or Atg5- silenced adipocytes whereas the expression level of NRF2 was increased by ULK1 or ULK2 knockdown (Fig. 20C). This result suggests that ULK1, ULK2 or Atg5 knockdown enhances the expression levels of a set of genes involved in mitochondria biogenesis and oxidative stress response which are crucial for ameliorating cellular stress caused by ROS and protein oxidation.

Knowing the effects of ULK1 and ULK2 on the expression levels of anti-oxidative stress genes, we sought to determine whether ULK1 and ULK2 regulate mitochondrial respiratory activities. We measured oxygen consumption rate (OCR) using XF24 bio-energetic assay instrument from Seahorse bioscience company (Fig. 21A) (Wu M 2007). Interestingly, the rest of tracing-respiration profile was dramatically changed by knockdown of ULK1, ULK2 or Atg5 compared to control shRNA transduction. We observed that the basal respiration is reduced and the non-mitochondrial respiration is increased by knockdown of ULK1, ULK2 or Atg5 (Fig. 21B and D). The mitochondria in ULK1, ULK2 or Atg5-silenced cells had a decreased response to oligomycin A (ATP coupler) compared to control cells (Fig. 21C), indicating that mitochondrial function was impaired with ULK1, ULK2 or Atg5 knockdown.

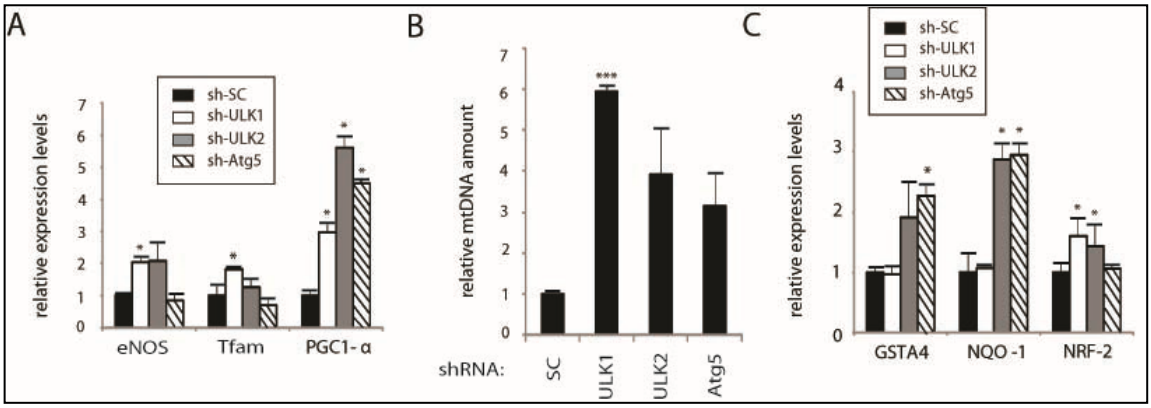

Figure 20. Knockdown of ULK1 or ULK2 increases expression of genes involved in mitochondrial biogenesis and oxidative stress response. (A) Expression of transcription factors and target mRNA in mitochondrial biogenesis. (B) Knockdown of ULK1, ULK2, or Atg5 enhanced mitochondrial DNA (mtDNA) content. Total DNA was purified from adipocytes and the amount of COX II mitochondrial DNA relative to nuclear DNA measured by quantitative PCR. Detailed procedures are described in Materials and Methods section. (C) Expression of target mRNA in oxidative stress response. Values are mean ± std. *, $p < 0.05$; **, $p < 0.01$; ***, $p < 0.001$.

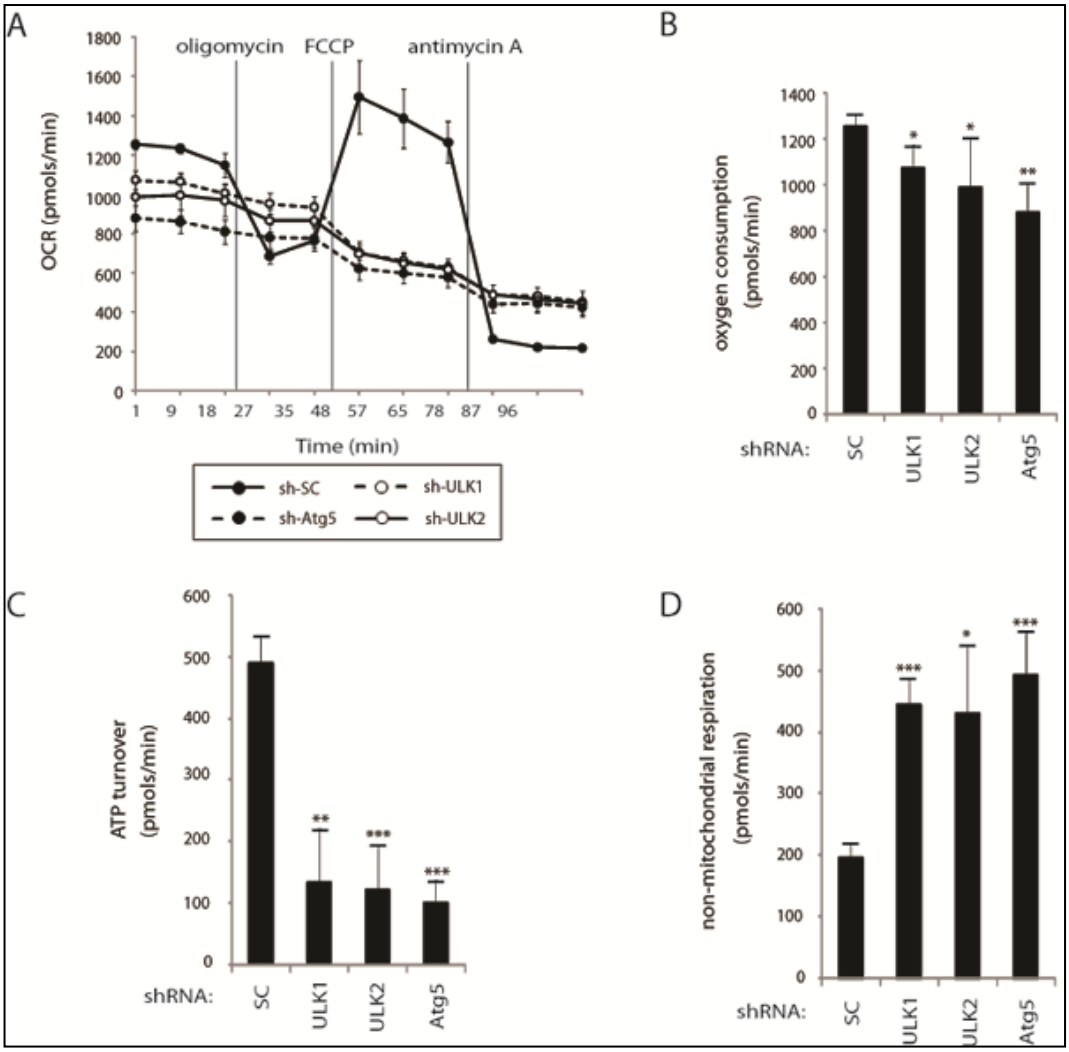
A
oligomycin
FCCP
antimycin A
OCR (pmols/min)
Time (min)
sh-SC
sh-ULK1
sh-Atg5
sh-ULK2
B
oxygen consumption (pmols/min)
shRNA:
SC
ULK1
ULK2
Atg5
C
ATP turnover (pmols/min)
shRNA:
SC
ULK1
ULK2
Atg5
D
non-mitochondrial respiration (pmols/min)
shRNA:
SC
ULK1
ULK2
Atg5

Figure 21. ULK1 or ULK2 are important for mitochondria respiration in adipocytes. (A) ULK1, ULK2 or Atg5 shRNA-transduced adipocytes were subjected to energy metabolism analysis using XF24 extracellular flux analyzer. (B) Knockdown of ULK1, ULK2 or Atg5 significantly reduced mitochondrial oxygen consumption rates. (C) Knockdown of ULK1, ULK2 or Atg5 significantly reduced ATP turnover rates. (D) Knockdown of ULK1, ULK2 or Atg5 enhances non-mitochondrial respiration. Values are mean ± std. *, $p < 0.05$; **, $p < 0.01$; ***, $p < 0.001$. Detailed procedures are described in Materials and Methods section.

4.4. ULK1 and ULK2 are important for protecting adipocytes from oxidative stress and apoptotic cell death.

Dysfunction of mitochondria is the major source of ROS and oxidative stress (Boudina S 2005; Scherz-Shouval R 2007; Kim JA 2008; Pauw AD 2009). Consistent with the reduced efficiency in the respiration and increased non-mitochondrial respiration (Fig. 21A and B), knockdown of ULK1 or ULK2 in adipocytes exhibited a significant increase in ROS (Fig. 22A). To confirm that the increase in the level of ROS is due to dysfunctional mitochondria, we isolated mitochondria from the cells and analyzed the level of ROS per mitochondria. Knockdown of ULK1, ULK2 or Atg5 enhanced the production of ROS per mitochondrion (Fig. 22B), suggesting that dysfunctional mitochondria contributed to the increase in the ROS. Knockdown of ULK1, ULK2 or Atg5 also increased protein carbonylation (Fig. 22C), a covalent modification reflecting protein oxidation (Grimsrud PA 2007). Increased carbonylation of specific proteins was noted in ULK1 and ULK2 knockdown relative to control adipocytes. The prominent band near ~15 kDa in adipocytes has previously been identified as the adipocyte fatty acid-binding protein (aP2) (Grimsrud PA 2007; Curtis JM 2010). Other proteins at 20, 30, 40, and 70 kDa (*) exhibited 2.8, 4.7 or 6.7 folds increase ($P < 0.05$) in carbonylation in the ULK1, ULK2 or Atg5 knockdown cells, respectively (Fig. 22C and D). Combined together, these results suggest that ULK1, ULK2 and Atg5 are important for mitochondrial functional maintenance thereby suppressing production of ROS and oxidative stress.

Knowing the crucial function of ULK1 and ULK2 in maintaining mitochondrial function and suppressing the production of ROS and oxidative stress, we inquired whether ULK1 and ULK2 would affect the capacity of adipocytes to respond to oxidative stress. We tested this possibility by incubating the shRNA-transduced adipocytes with tumor necrosis factor α (TNFα), the cytokine that induces oxidative stress in adipocytes (Chen XH 2010; Curtis JM 2010). Knowing that ROS and oxidative stress can cause impairment in insulin action via activation of p38 mitogen activated protein kinase (MAPK) and inhibitor kappaB kinase-beta (IKK2)/NF-kB pro-inflammatory signaling (Yuan M 2001; Gao Z 2002; Carlson CJ 2003; Evans JL 2003; de Alvaro C 2004; Nieto-Vazquez I 2008; Zhang J 2008; Yang J 2009), we investigated whether knocking down any of the autophagy genes could increase the pro-inflammatory pathway activities. We found that knockdown of ULK1, ULK2, or Atg5 increased the phopshorylation of p38 MAPK at Thr180/Tyr182 and processing of NF-kB1 into p50 (Fig. 23). This result suggests that autophagy is important to suppress pro-inflammatory signaling under oxidative stress. Consistent with these results, cell death was increased in cells where ULK1, ULK2 or Atg5 was knocked down compared to control cells (Fig. 24). This result would support that autophagy is important for adipocytes to survive under oxidative stress.

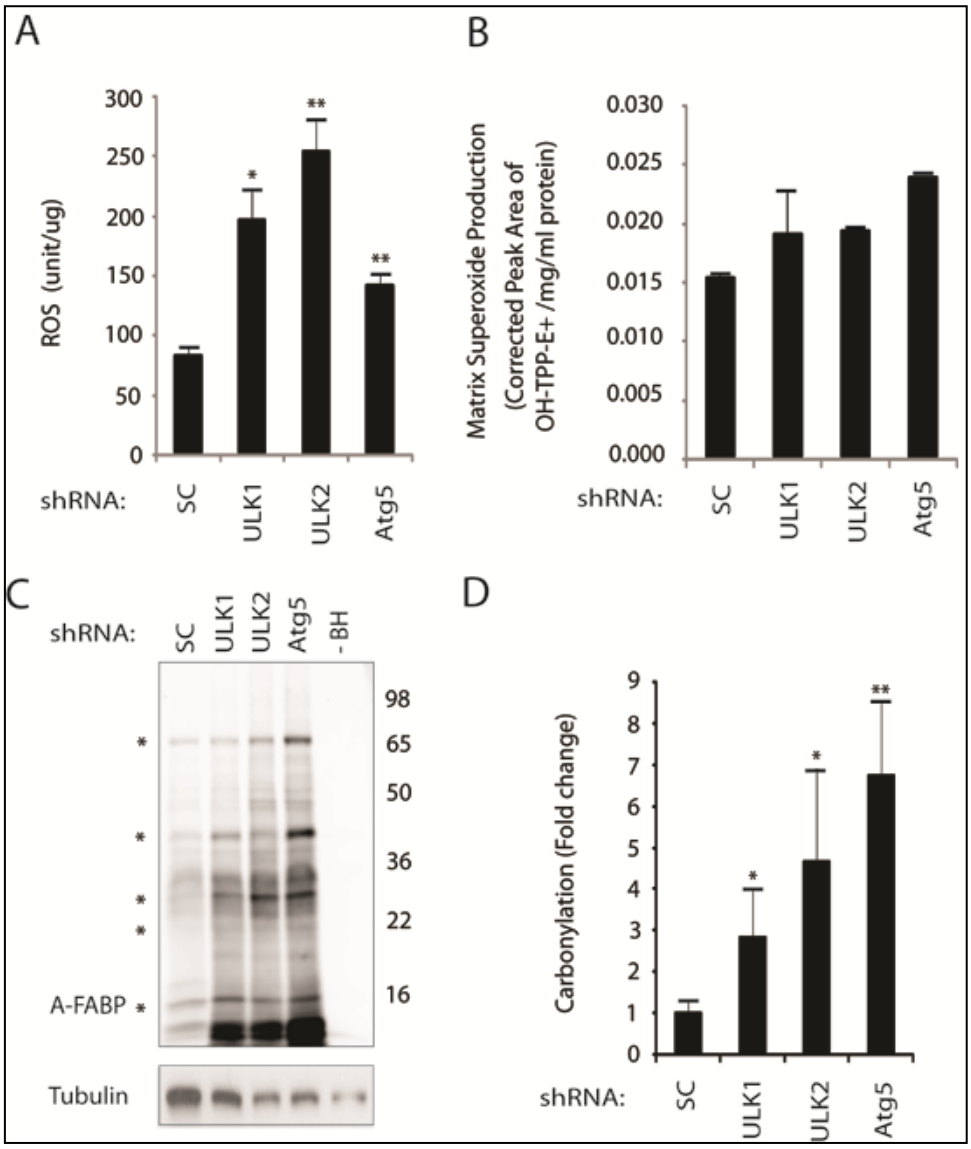
A
ROS (unit/ug)
300
250
200
150
100
50
0
*
**
**
shRNA:
SC
ULK1
ULK2
Atg5
B
Matrix Superoxide Production
(Corrected Peak Area of
OH-TPP-E+ /mg/ml protein)
0.030
0.025
0.020
0.015
0.010
0.005
0.000
shRNA:
SC
ULK1
ULK2
Atg5
C
shRNA:
SC
ULK1
ULK2
Atg5
- BH
98
65
50
36
22
16
A-FABP
Tubulin
D
Carbonylation (Fold change)
9
8
7
6
5
4
3
2
1
0
*
*
**
shRNA:
SC
ULK1
ULK2
Atg5

Figure 22. ULK1 and ULK2 are important for suppressing oxidative stress accumulation in adipocytes. (A) Fluorescent probe H_2DCFDA was used for whole-cell ROS detection in differentiated 3T3-L1 cells (day 8). (B) Matrix superoxide was measured in isolated mitochondria using TPP-HE. (C) Knockdown of ULK1, ULK2 or Atg5 increased carbonylation of proteins. Carbonylation of adipocyte proteins was analyzed by use of EZ-link Biotin Hydrazide (BH). Lane with no BH label is used as a control for background carbonylation level. (D) Quantitative analysis of protein carbonylation. The values were obtained from the band intensities for proteins of molecular sizes of 15, 20, 30, 40, and 70 kDa. Values are mean ± std. *, $p < 0.05$; **, $p < 0.01$. Detailed procedures are described in Materials and Methods section.

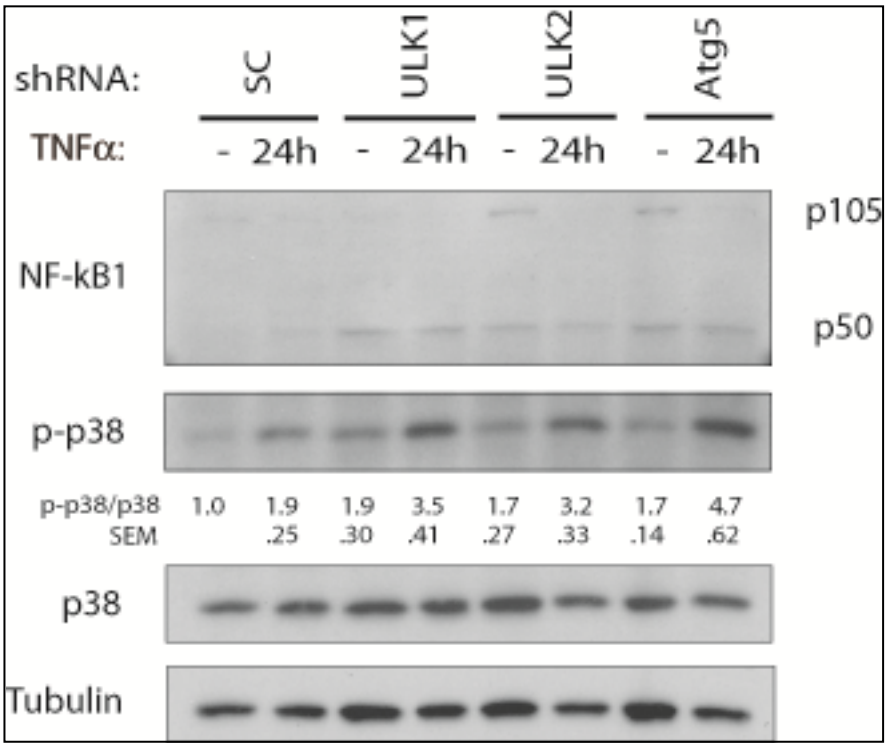

Figure 23. Autophagy is important to suppress pro-inflammatory signaling under oxidative stress. Knockdown of ULK1, ULK2 or Atg5 increased pro-inflammatory signaling. Cell lysate was obtained from adipocytes at day 10 after induction of differentiation in RIPA buffer after treating 20 μM TNFα for 24 hr. NF-kB1 processing (p105 → p50) and the phosphorylation state of p38 MAPK at Thr180/Tyr182 were analyzed by Western blotting.

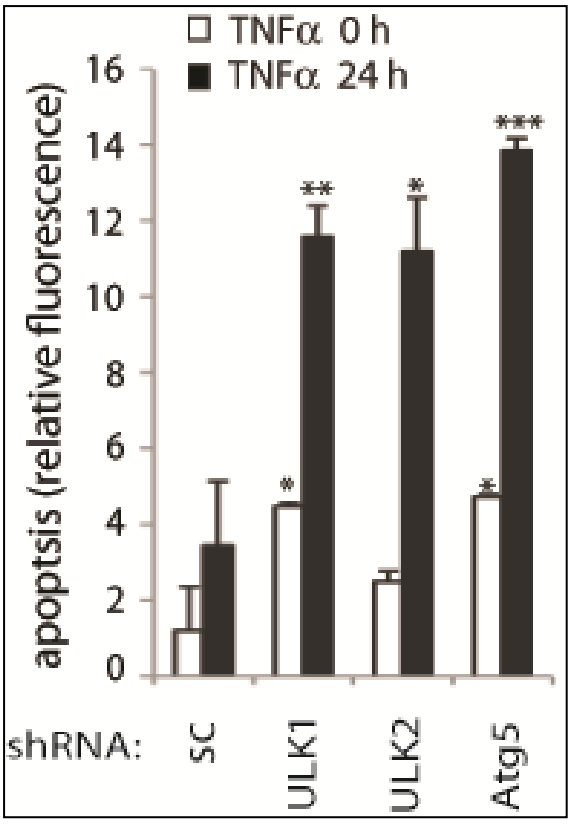

Figure 24. Knockdown of ULK1, ULK2 and Atg5 increased cell death activities. Knockdown of ULK1, ULK2 or Atg5 enhanced apoptosis of adipocytes. Differentiated 3T3-L1 cells (day 8) were treated with TNFα and then the cell death activity was measured by using APO-BrdU TUNEL (Terminal deoxynucleotide transferase dUTP nick end labeling) Assay kit. Values are mean ± std. *, $p < 0.05$; **, $p < 0.01$; ***, $p < 0.001$. Detailed procedures are described in Materials and Methods section.

4.5. Conclusion

My study revealed that knockdown of ULK1 or ULK2 in 3T3-L1 adipocytes inhibited mitochondrial respiration, which was accompanied by increases in oxidative stress, pro-inflammatory signaling and apoptotic cell death. I also found that ULK1 and ULK2 negatively regulate mTORC1 signaling. Knockdown of ULK1, ULK2 or Atg5 reduced ATP production from mitochondria and increased glycolysis. ULK1 knockdown enhanced ROS and oxidative stress, which are known key factors contributing to insulin resistance (Nishikawa T 2007). Furthermore, ULK1 knockdown facilitated cell death under a prolonged stress condition such as TNFα treatment over 24 h. This result suggests that autophagy might be important for adipocytes to survive under oxidative stress. In conclusion, ULK1 and ULK2 share key functions in lipolysis, mitochondrial respiration and protection of cells against oxidative stress.

The outcomes suggest that ULK1 knockdown has both beneficial and harmful effects on adipocyte metabolism and function. The beneficial effect may involve an increase of insulin-stimulated glucose uptake, whereas the harmful effects involve induction of oxidative stress and apoptotic cell death under stress conditions. These functions of ULK1 might be relied on ULK2, since ULK2 is up-regulated in ULK1-silenced adipocytes and it has a dominant effect over ULK1 in the regulation of adipogenesis.

CHAPTER 5 : Discussion

My study has demonstrated that ULK1 and ULK2 have distinct functions in the regulation of metabolism in adipocytes (Fig. 25). This result appears to be distinct from the previously-known function of autophagy role in adipogenesis (Baerga R 2009; Singh R 2009; Zhang Y 2009; Goldman S 2010; Kovsan J 2011). A possible interpretation for the different effects might be that ULK1 has a unique function of ULK1 in adipogenesis. However, we note that autophagy was not completely suppressed in the knocked-down cells. Thus, one would assume that a basal level of autophagy might be necessary and sufficient for differentiation while ULK1 negatively regulating differentiation through an unknown mechanism. Knockdown of both ULK1 and ULK2 showed that ULK2 effect is dominant over ULK1 effect on adipogenesis. Thus, ULK2 is an important component that may constitute the autophagy pathway crucial for adipogenesis. This pathway may involve Atg5/Atg7 but not ULK1. We wonder how autophagy is still inhibited, even though ULK1 expression was dramatically increased in ULK2-silenced adipocytes. This implies that the up-regulation of ULK1 would not necessarily contribute to autophagy. A possible explanation is that ULK1 at extra amounts may not be in a functional complex with its binding partners. Alternatively, ULK2 may have a unique function in the autophagy pathway.

ULK2 and Atg5 showed similar effects not only on adipogenesis but also on most of other metabolic parameters. Knockdown of ULK2 or Atg5 in adipocytes inhibited

adipogenesis and enhanced fatty acid oxidation (Fig. 13 and 16B). This result is consistent with what was observed with Atg7 deficiency or knockdown (Nishida Y 2009; Singh R 2009; Zhang Y 2009). It is unclear how ULK1 and ULK2 have different effects on fatty acid oxidation and fatty acid synthesis. The increase in fatty acid oxidation by ULK2 or Atg5 knockdown, despite the reduction in the mitochondrial respiration, could be possible due to the increase in the content of mitochondria that still maintain the intact machinery for fatty acid oxidation. The increase in glucose uptake may be accompanied by glycolysis and fatty acid synthesis with reduced lipolysis and fatty acid oxidation. Alternatively, ULK1 knockdown might specifically suppress the expression of genes involved in fatty acid oxidation. According to the change in gene expression, it appears that ULK1 and ULK2 regulate different sets of genes involved in fatty acid metabolism. PPAR-γ is likely an important transcription factor involved in the different effects by knockdown of ULK1 or ULK2. ULK1 and ULK2 have not only distinct but also similar functions in the regulation of adipocyte metabolism. Knockdown of ULK1 or ULK2 enhanced the activity of mTORC1 signaling (Fig. 18A and B). Although ULK1 and ULK2 have the shared function in negatively regulating mTORC1 signaling, only the knockdown of ULK1 enhanced the expression levels of IRβ and IRS-1 (Fig. 18A and B). Atg5 knockdown also had a positive effect on mTORC1 activity, which is different from what was observed with other cell types (Lee SB 2007; Dunlop EA 2011; Jung CH 2011). This finding suggests that mTORC1 signaling might not be responsible for the opposing effects of ULK1 and ULK2 on

adipogenesis and possibly up-regulation of IRβ and IRS-1 might have contributed to the higher level of adipogenesis in ULK1-silenced cells.

Knockdown of ULK1, ULK2 or Atg5 reduced ATP production from mitochondria and increased the level of GLUT1, basal glucose uptake and glycolysis (Fig. 19A, C, and D; Fig. 21C). The down-regulation of fatty acid oxidation, mitochondrial respiration and lipolysis and the up-regulation of glucose uptake are well known to correlate with mitochondrial dysfunction (Lowell 2005). Why would autophagy-defective adipocytes become more dependent on glycolysis which is less efficient in producing energy? This might be related to accumulation of damaged mitochondria. Autophagy-defective adipocytes may depend less on mitochondria but more on glycolysis to produce energy. Through such a metabolic change, adipocytes may avoid further accumulation of the ROS and oxidative stress. ULK1 showed a distinct effect from ULK2 and Atg5 in the regulation of GLUT4 expression and insulin-sensitive glucose uptake. The increase in insulin-stimulated glucose uptake might be potentially related to the up-regulation of GLUT4, IRβ and IRS-1 (Fig. 18A and B; Fig. 19D). The increase in the levels of IRβ and IRS-1 in ULK1-silenced adipocytes did not contribute to an increase in Akt activation (Fig. 18). Thus, if IRβ and IRS-1 contributed to insulin-stimulated glucose uptake, it must be through a mechanism independent of Akt. Although the result above supports a function of ULK1 in the regulation of insulin-stimulated glucose uptake in adipocytes, ULK1 knockdown enhanced ROS and oxidative stress (Fig. 22 and 23), which are known key factors contributing to insulin resistance (Nishikawa T 2007).

Furthermore, ULK1 knockdown facilitated cell death under a prolonged stress condition such as TNFα treatment over 24 h (Fig. 24). Thus, ULK1 knockdown has both beneficial and harmful effects on adipocyte metabolism and function. The beneficial effect may involve an increase of insulin-stimulated glucose uptake, whereas the harmful effects involve induction of oxidative stress and apoptotic cell death under stress conditions. These functions of ULK1 might be relied on ULK2, since ULK2 is up-regulated in ULK1-silenced adipocytes and it has a dominant effect over ULK1 in the regulation of adipogenesis.

According to our study, the increase in the activity of adipocyte autophagy in diabetic and obese states (Zhang Y 2009; Zhou L 2009; Ost A 2010; Kovsan J 2011) could be due to a cellular protective mechanism against the metabolic stress, rather than due to any causative effect of autophagy on the development of such disease states. This protective function of autophagy might be important especially when adipocytes are under metabolic stress. Given the opposing effects and the reciprocal compensatory relation between ULK1 and ULK2, a currently-unknown mechanism might exist to coordinately regulate the ULK1- and ULK2-dependent pathways to determine insulin sensitivity and stress response of adipocytes. Further studies on the function of ULK1 and ULK2 in adipocytes might provide important insight into the role of ULK and autophagy in the pathophysiology of obesity and related diseases.

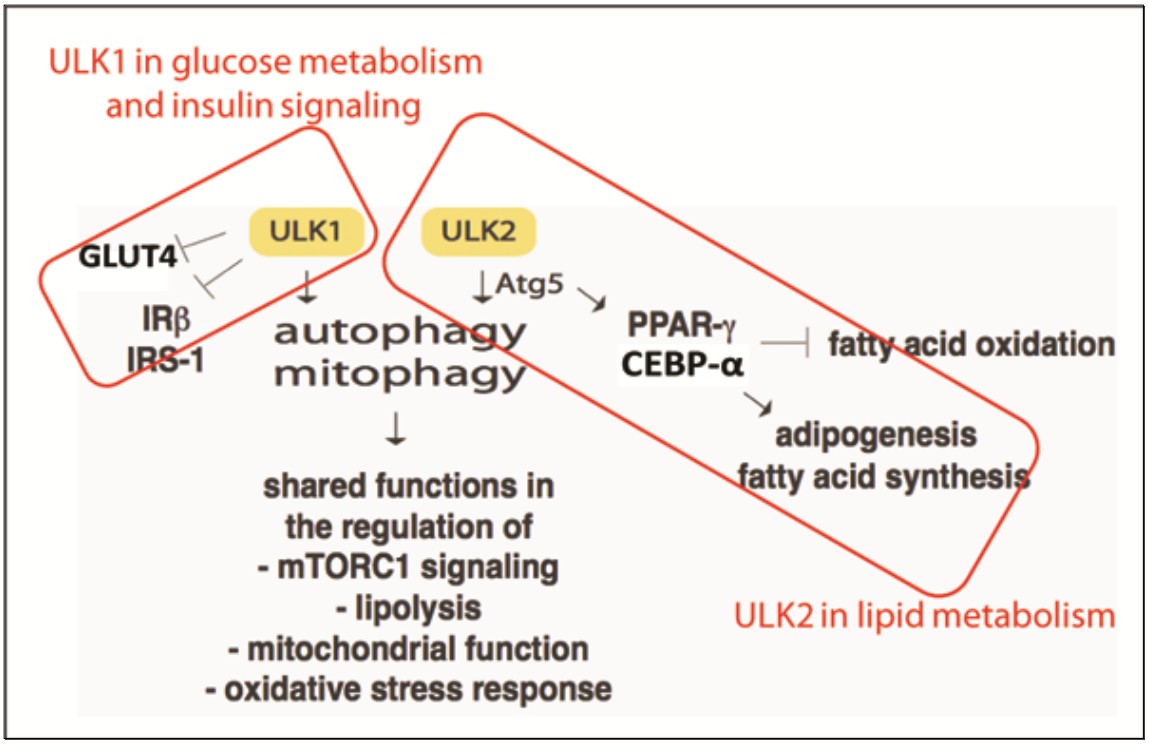
ULK1 in glucose metabolism
and insulin signaling
GLUT4
ULK1
IRβ
IRS-1
autophagy
mitophagy
shared functions in
the regulation of
- mTORC1 signaling
- lipolysis
- mitochondrial function
- oxidative stress response
ULK2
Atg5
PPAR-γ
CEBP-α
fatty acid oxidation
adipogenesis
fatty acid synthesis
ULK2 in lipid metabolism

Figure 25. A summary for the role of ULK1 and ULK2 kinases in adipocyte metabolism. ULK1 and ULK2 have shared functions in the regulation of mTOC1 signaling, lipolysis, mitochondrial function, and oxidative stress response through autophagy or mitophagy. On the other hand, ULK1 has distinct functions in the regulation of glucose metabolism and insulin signaling by inhibiting GLUT4, IRβ, and IRS-1 whereas ULK2 has distinct function in the regulation of lipid metabolism by positively regulating adipogenesis and fatty acid synthesis and negatively regulating fatty acid oxidation through PPAR-γ and CEBP-α. This result also suggests that ULK2, rather than ULK1, is more closely related to Atg5 in adipocytes. In sum, this study provided the distinct and shared functions between ULK1 and ULK2 in comparison with Atg5 in adipocyte metabolism.

CHAPTER 6 : Future directions

Although this study has provided important insight into the role of ULK and autophagy in the regulation of adipogenesis and adipocyte metabolism, there remain many questions with respect to the underlying mechanisms. How ULK1 negatively regulates adipogenesis? How could ULK1 and ULK2 be distinctly regulated? Is this function related to autophagy or not? How can this study and the obtained knowledge be useful to develop therapeutics for diabetes and obesity?

Given the distinct functions between ULK1 and ULK2, a study to identify their unique substrates might be important to elucidate the mechanisms differently regulated by the two kinases. Knowing that PPAR-γ is differently regulated by ULK1 and ULK2 (Fig. 13C), it would also be interesting to investigate what is the underlying mechanism that leads to the difference in the regulation. PPAR-γ is regulated by PGC-1α, which is the coactivator of PPAR-γ, inducing gene expressions of adipocyte differentiation and increasing mitochondria mass and function (Liang H 2006; Medina-Gomez G 2007; Tontonoz P 2008). It might be possible that ULK1 and ULK2 regulate these transcriptional factors through phosphorylation of currently-unknown intermediate molecules that regulate the transcriptional factors.

In future studies, mouse models would be important to understand the physiological meaning of our findings. Currently, ULK1 KO mouse model is available. ULK1 fl/fl

mice are also available and have been used to generate adipose specific ULK1 KO mice. These mice would be important resources in addressing the questions imposed above and providing important insight into the physiological roles of these kinases and adipocyte autophagy in the regulation of adipose metabolism. These mice would also allow us to investigate how ULK1- or ULK2-regulated autophagy in adipose tissue regulates energy metabolism in peripheral tissues and the whole body level. Ultimately, these studies may contribute to better understanding of the function of autophagy in obesity and insulin resistance.

CHAPTER 7 : Materials and Methods

Mouse tissue sample preparation. Male mice strain C57BL/6J were fed normal chow (~ 4% fat by weight, Teklad) or high fat diet (~35 % fat by weight, F3282, BioServ) at weaning (Surwit RS 1988). Mice were housed on a 12-h light/dark cycle and fed ad libitum with continual access to water. At 12 weeks of age, they were weighing 34-49 g and 26-33 g, respectively. Each group of mice were fasted for 4 h and euthanized by carbon dioxide, and epididymal white adipose tissues were excised. Fat tissue were immediately frozen in liquid nitrogen and stored at -80 °C until further processing. The University of Minnesota Institutional Animal Care and Use Committee approved all experiments.

Antibodies and chemicals. Primary antibodies were from the following sources: anti-insulin receptor β (3025), anti-insulin receptor substrate-1 (IRS-1, 2382), anti-Akt (9272), anti-phospho-Akt (9271), S6K1 (9202), anti-phospho-S6K1 (9205) and anti-p38 (9212) from Cell Signaling Tech (Danvers, MA); anti-CEBP-α (sc-61), anti-PPAR-γ (sc-7196), anti-GAPDH (sc-25778), anti-tubulin (sc-12462) from Santa Cruz Biotech. (Santa Cruz, CA); anti-Atg5 antibody (110-53818) from Novus Biologicals (Littleton, CO); anti-ULK1 (A7481) from Sigma-Aldrich; anti-β-actin (612657) from BD Biosciences; anti-GLUT4 (AB1346) from Chemicon. GLUT1 antibody was kindly provided by Dr. Xiaoli Chen (University of Minnesota). Chemicals were purchased from the following sources: rapamycin (553210, EMD Chemicals); insulin (I6634),

methylisobutylxanthine (I5879), dexamethasone (D4902), troglitazone (T2573), Oil Red O (0625), pepstatin A (P5318), cytochalasin B (C6762), puromycin (82595), forskolin (F3917), and E-64 (E3132) from Sigma-Aldrich; 4,4-difluoro-5-methyl-4-bora-3a,4a-diaza-s-indacene-3-dodecanoic acid (BODIPY) (D3823), DAPI (D1306), chloromethyl 2',7'-dichlorodihydrofluorescein diacetate (H_2DCFDA) (C6827), TRIzol reagent (15596-018), APO-BrdU Terminal deoxynucleotidyl transferase dUTP nick end labeling (TUNEL) Assay kit (A35125 and A35126), LysoTracker Red (L7528) from Invitrogen; EZ-link Biotin Hydrazide (21339, Pierce); NEFA-HR (999-34691,995-34791,991-34891, and 993-35191) from Wako diagnostics; Oligomycin A, Carbonyl cyanide 4-(trifluoromethoxy) phenylhydrazone (FCCP), and antimycin A from Seahorse Bioscience (101706-110); RNase free DNAse I (AM2222, Ambion); iScript cDNA Synthesis Kit (170-8891) and iQ SYBR Green Supermix (170-8880) from Bio-Rad; 2.5 % glutaraldehyde, sodium cacodylate, Osmium tetroxide, tannic acid, ethanol: embed 812 resin, and 20 mm gelatin capsules from Electron Microscopy Sciences (Hatfield, PA); Mouse tumor necrosis factor α (mTNFα) (5178) from Cell Signaling Tech (Danvers, MA).

Quantitative real-time RT-PCR. Total RNAs from isolated adipose cells from mouse epididymal fat depot, 3T3-L1 adipocytes were extracted using TRIzol reagent (15596-018, Invitrogen, Carlsbad, CA) according to the manufacturer's instructions. RNA was treated with RNase free DNAse I (AM2222, Ambion) at 37ºC for 30 min, followed by extraction with phenol-chloroform and ethanol precipitation. The first-strand cDNA was

generated using iScript cDNA Synthesis Kit (170-8891, Bio-Rad, Hercules, CA) was used in each 20 µl real-time PCR reaction using the iQ SYBR Green Supermix (170-8880, Bio-Rad) with ICycler Real Time PCR System (Bio-Rad). Primers specific for the examined genes are listed (Table 1). β-Actin or TFIIE was selected as an internal standard. Results were analyzed using iQ5 software supplied with the ICycler system. All raw data are expressed as the ratio of the selected gene to standard. Statistical significance was determined by two-tailed Student's t test.

Lentiviral preparation, viral infection and stable cell line generation. Oligonucleotides for sh-RNA targeting GFP scrambled, ULK1, ULK2, and Atg5 were annealed and cloned into pLKO shRNA vectors (Table 2). Lentiviral stocks were produced by transfecting pLKO shRNA vectors with lentiviral packaging vectors pHR'8.2ΔR and pCMV-VSV-G using Fugene 6 (Invitrogen) into HEK-293T cells. Supernatants were harvested over 60 hours. 3T3-L1 cells grown on 6-cm dishes were infected with collected viruses four times over 15 h in the presence of polybrene (Sigma-Aldrich). Selection for cells transduced by shRNA lentiviruses to knockdown endogenous mouse ULK1, ULK2 or Atg5 was performed in the presence of 2.5 µg/ml puromycin (82595, Sigma-Aldrich). Expression levels of ULK1 or Atg5 in stable cell lines were analyzed on western blots using anti-ULK1 or anti-Atg5 antibodies. ULK2 knock down was confirmed by RT-PCR.

Adipocyte differentiation, lipid staining, and triglyceride measurements. 3T3-L1 preadipocytes were cultured and differentiated into adipocytes as described previously (Student AK 1980). Preadipocytes were cultured in DMEM containing 10 % calf serum. Two days after reaching confluence, cells were induced to differentiate in DMEM supplemented with 10 % FBS, 174 μM insulin (I6634, Sigma-Aldrich), 0.5 mM methylisobutylxanthine (I5879, Sigma-Aldrich), and 0.25 μM dexamethasone (D4902, Sigma-Aldrich). Two days after initiation of differentiation, dexamethasone and methylisobutylxanthine were withdrawn from the medium, whereas insulin was withdrawn after 4 days. Differentiated adipocytes were maintained in DMEM and 10 % FBS until mature (days 8-10). For full differentiation of autophagy gene silenced 3T3-L1 cells, 5 μM troglitazone (T2573, Sigma-Aldrich) was treated along with differentiation inducing chemicals, and then lipid droplets were stained using Oil Red O (0625, Sigma-Aldrich) solutions. To measure intracellular triglyceride levels, Oil Red O was extracted from cells with isopropanol, and optical density was then measured at a wavelength of 490 nm. Triglyceride levels were normalized to protein concentration.

Microscopic analysis of autophagosome formation. GFP scrambled, ULK1 Kd, ULK2 Kd and Atg5 Kd 3T3-L1 preadipocytes were seeded onto glass coverslips and differentiated into adipocytes as described previously (Curtis JM 2010). On day 8, Autophagy was induced by 100 nM rapamycin (44532-U,Sigma-Aldrich) or vehicle (DMSO) in the presence of pepstatin A (P5318,Sigma-Aldrich) and E-64 (E3132, Sigma-Aldrich) (10 μg/ml each), an inhibitor of the lysosomal protein degradation. After

5 h of induction, cells were fixed with formaldehyde, permeabilized using 1 % Triton X-100, and stained with anti-LC3 antibody (100-2220) from Novus and 4, 6-diamidinophenylindole (DAPI) from Invitrogen (D1306). Cells were visualized under a confocal microscope attached IX70 inverted microscope (Olympus, Center Valley, PA). Multiple fields at random positions were collected for each condition. Quantification of LC3-labeled structures in the images was performed by counting the number of cells with LC3-positive structures (Klionsky DJ 2008; Klionsky DJ. 2008).

Western blot assay of autophagy. 3T3-L1 adipocytes were incubated with rapamycin for 5h in the presence of pepstatin A and E-64 (10 μg/ml each). Cell lysates were obtained and run on SDS-PAGE and transferred to polyvincylidene difuoride membranes and probed with anti-LC3 mouse polyclonal antibody (Nanotools, France) and anti-p62 antibody (610832, BD Biosciences).

Immunoblot analysis. For analysis of proteins in autophagy and insulin signaling, adipose cells was lysed in RIPA buffer (50 mM Tris-HCl pH 7.4, 10 mM $MgCl_2$, 500 mM NaCl, 1 % Triton X-100, 0.1 % SDS, 0.5 % deoxycholate, and protease inhibitors [Complete; Boehringer Mannheim]) followed by centrifugation (13000 rpm; 10 min; 4ºC). Protein content of supernatants was determined using the BCA kit (Thermo Scientific). A total of 30 μg protein was analyzed by immunoblotting for expression of autophagy proteins (ULK1, Atg5), insulin signaling proteins [IRβ, IRS-1, Akt, p-Akt,

S6K1, p-S6K1] by antibodies purchased from previously noted companies. Insulin was dissolved in 0.02 N HCl for treatment (I6634, Sigma-Aldrich).

Electron microscopy imaging. Cells on thermonox cover slips (Thermo Scientific, Rochester, NY, USA) were fixed in 1 ml of 2.5 % glutaraldehyde in 0.1 M sodium cacodylate buffer in 6 well plates overnight at 4°C. The cells on thermonox cover slips were washed three times with 0.1 M sodium cacodylate buffer and post fixed with 1% osmium tetroxide in 0.1 M sodium cacodylate buffer. Followed by incubation in 1% tannic acid, these samples were washed in distilled water and dehydrated using a 25-100 % ethyl alcohol gradient. Samples were then infiltrated with 2:1 ethanol: Embed 812 resin for 1 hour and subsequently transferred to a 1:2 ethanol: Embed 812 resin mixture for 1 hour. Cells on thermonox cover slips were infiltrated with 100 % resin and were embedded on top of 20 mm gelatin capsules and incubated at 58^{o}C for 24 hours to polymerize the resin. Embedded samples were trimmed and sectioned on a Leica UC6 Ultramicrotome (Leica Microsystems, Vienna, Austria). Thin sections (60-70 nm) were obtained and collected on a 200 mesh copper grid (Electron Microscopy Sciences, Hatfield, PA, USA) using a perfect loop. Grids were stained with 5% uranyl acetate for 20 minutes and Satos' lead citrate for 6 minutes. These sections were observed in the JEOL 1200 EX II transmission electron microscope (JEOL LTD, Tokyo, Japan). Images were obtained using a Veleta 2K x 2K camera with iTEM software (Olympus SIS, Munster, Germany). The autophagosome structures indicated by red arrows were visually identified with characteristics of protein aggregates or cellular compartments

within double membrane-structures. The total number of autophagosomes of 10 randomly selected cells was counted. In each cell, up to 10 autophagosomes were randomly selected and their perimeter and area were measured and recorded using the iTEM software (Olympus SIS).

Glucose uptake assay. 3T3-L1 adipocytes were serum-starved in Krebs–Ringer's Hepes buffer (130 mM NaCl, 5 mM KCl, 1.3 mM $CaCl_2$, 1.3 mM $MgSO_4$, and 25 mM Hepes pH 7.4) supplemented with 0.5 % BSA and 2 mM sodium pyruvate (pH 7.4) and incubated either with or without 100 nM insulin for 1 hr at 37°C. Glucose uptake was initiated by the addition of [^{3}H]-2-deoxy-D-glucose (PerkinElmer Life and Analytical Sciences, Boston, MA) to a final assay concentration of 100 μM at 37ºC. After 5 min, 2-deoxyglucose uptake was terminated by three washes with ice-cold Krebs-Ringer's Hepes buffer, and the cells were solubilized with 0.8 ml of Krebs-Ringer's Hepes buffer containing 1 % Triton X-100. The incorporated radioactivity was determined by scintillation counting. Nonspecific 2-deoxyglucose uptake was measured in the presence of 20 μM cytochalasin B (C6762, Sigma-Aldrich) and subtracted from the total glucose uptake assayed to determine specific uptake (Lobo S 2007).

Lipolysis assay. To evaluate lipolysis, 3T3-L1 adipocytes were washed with phosphate-buffered saline (PBS) and incubated at 37ºC in KRH supplemented with 2 % fatty acid-free BSA and 5 mM glucose with or without 40 μM forskolin. Media was collected after one hour and the non-esterifed fatty acids determined using the NEFA-HR (Student AK

1980) assay according to the manufacturer's instructions (Wako Diagnostics, Mountain View, CA, USA).

Microscopic analysis for autophagic clearance of lipid droplets. 3T3-L1 preadipocytes cells seeded onto glass coverslips. After fully differentiated (day 8), medium was refreshed with serum free DMEM or DMEM containing 10% FBS serum. Macroautophagy was induced by serum starvation in the presence of pepstatin A and E-64 (10 μg/ml each), an inhibitor of the lysosomal protein degradation (Sigma). After 2h of induction, cells were fixed with formaldehyde, permeabilized using 1% Triton X-100 for 15 min at RT. Lysosomes were stained with 100 nM lysotracker Red (Invitrogen) for 30 min at RT, then lipid droplets were labeled with 1 μg/ml BODIPY 493/503 (Molecular probes) and nucleus were labeled with 4, 6-diamidinophenylindole (DAPI) each for 1 min at RT. Glass coverslips were washed with PBS three times. Engulfment of lipid droplets by autophagosome were visualized under high magnification (100X) of a confocal microscope attached IX70 inverted microscope (Olympus).

Fatty acid β-oxidation. 3T3-L1 adipocytes were serum-starved for 2h, and subsequently incubated in DMEM containing 5.4 mM glucose, 4 mM glutamine, 1% fatty acid-free BSA, and 0.25 mM oleate. β-oxidation was initiated upon addition of 0.2 mM [1-^{14}C]-oleic acid (0.8 μCi/ml) buffered with 1% FA-free BSA and incubated for 90 min at 37 ºC and 5% CO_2 (Lobo S 2007). Each well was covered immediately by a piece of square shape Whatman paper. After incubation, 150 μl of 3 M NaOH was added

on the paper and then 70 % perchloric acid was injected into wells. Filter papers containing trapped CO_2 from each well were transferred to liquid scintillation fluid and $^{14}CO_2$ content was determined.

Mitochondrial DNA quantification. To determine mitochondria DNA levels, total genomic DNA was isolated with DNAzol reagent (Invitrogen), and the amount of mtDNA was compared with nuclear DNA. mtDNA copy number was measured by means of quantitative PCR of mtDNA gene cytochrome C oxidase II (COXII) compared to the nuclear gene as described ((Piantadosi CA 2006; Grimsrud PA 2008)). mtDNA copy number was calculated by taking the absolute value of ΔCt values between groups (scrambled vs. knockdown).

Respiration of mitochondria and glycolysis. Oxygen consumption rate (OCR) and Extracellular acidification rate (ECAR) in scrambled, ULK1, ULK2 or Atg5 silenced adipocytes were measured by XF24 bioenergetic assay (Seahorse Bioscience, Billerica, MA, USA). Assays have been previously described in detail (Wu M 2007). Oligomycin A, Carbonyl cyanide 4-(trifluoromethoxy) phenylhydrazone (FCCP), and Antimycin A were purchased from Seahorse Bioscience (101706-110, XF cell mito-stress test kit, Seahorse Bioscience).

Measurement of intracellular ROS. Intracellular ROS levels were measured using the chloromethyl 2',7'-dichlorodihydrofluorescein diacetate (CM-H_2DCFDA) (C6827,

Invitrogen), a cell permeable nonfluorescent precursor. This dye measures H_2O_2, ROO^-, and $ONOO^-$. Within the cells, CM-H_2DCFHDA is hydrolyzed by nonspecific esterases to release CM-H2DCF, which is readily oxidized by intracellular ROS. The oxidized product emits green fluorescence with a wavelength of 516 nm after excitation with a wavelength of 492 nm (Ex.492/Em.516). The protocol was modified from manufacture's instruction. Briefly, ULK1, ULK2 or Atg5 silenced preadipocytes were cultured and differentiated on 24 well microplates (PerkinElmer). 3T3-L1 adipocytes (day 8) were loaded with 5 μM of fluorescent probe CM-H_2DCFDA for 30 min at 37ºC. Cells without fluorescent probe were used as control. Cells were washed with PBS three times before measurement. The fluorescence intensity was measured by VICTOR^{3}V Multilabel Counter 1420 (PerkinElmer). The measured values were normalized by protein concentration. All experiments were performed in triplicate.

Mitochondria isolation and matrix superoxide measurement. 3T3-L1 adipocytes were collected and incubated for 20min on ice in 20mM Tris pH 6.8 and 1 mM EDTA containing protease inhibitors. Cells were lysed with 40 strokes of a Dounce homogenizer, and the resulting homogenate was supplemented with a final concentration of 220 mM mannitol and 70 mM sucrose. For mitochondrial isolation from adipocytes, cells were washed in ice-cold Krebs-Ringer's Hepes, and lysed with 1:5 wt/vol of isolation buffer (20 mM Tris-HCl, 220 mM mannitol, 70 mM sucrose, 1 mM EDTA, pH 7.4 supplemented with protease inhibitors) by Dounce homogenization. Homogenates were centrifuged at 700g to remove nuclei, unbroken cells, and the lipid cake.

Mitochondria were recovered by centrifugation at 12,000g. TPP-HE was used to detect superoxide in isolated mitochondria as described previously (Xu X 2009). Superoxide level was normalized to mitochondrial protein.

Protein carbonylation. Protein carbonylation was detected using EZ-link Biotin Hydrazide (21339, Pierce, Rockford, IL) as described previously (Grimsrud PA 2007), with slight modifications. Polyvinylidene fluoride membranes (Millipore, Billerica, MA) were blocked in Odyssey Blocking Buffer (LI-COR, Lincoln, NE), and biotinylated proteins were detected with DyLight 800-conjugated streptavidin (Pierce) and visualized using an Odyssey Infrared Imager (LI-COR).

Apopotsis assay. APO-BrdU TUNEL (Terminal deoxynucleotide transferase dUTP nick end labeling) Assay kit was purchased from Invitrogen (A35125 and A35126). 3T3-L1 adipocytes (day 8) were treated with 20 μM TNFα for 24h. Then cells were washed with PBS and fixed with paraformaldehyde in PBS for 15 min on ice. Then cells were washed with cold PBS twice and stored in 70% Ethanol at -20ºC for 24h. Cells then washed twice with washing buffer followed by incubation with DNA-labelling solution (containing reaction buffer, terminal deoxynucleotidyl transferase (TdU), BrdUTP with dH_2O) for 60 min in 37ºC incubator, followed by 30 min incubation with Alexa fluor 488 dye-labeled anti-BrdU antibody (1:20 dilution) as previously described (Lin J 2004). Labeled cells were washed with PBS three times, and the fluorescence excitation and emission (492 nm/516 nm) were measured using VICTOR3 V Multilabel Counter model

1420 (PerkinElmer). The measured values were normalized by protein concentration. All experiments were performed in triplicate.

Statistical analysis. All values are expressed as mean ± standard deviation (std.). Statistical significance was determined by the two-tailed Student t test assuming unequal variances using Microsoft Office Excel or Sigma Plot (Jandel Scientific). *P* values < 0.05 are considered significant (*) with an increased significance of *P* value < 0.01 indicated (**) or *P* value < 0.001 indicated (***).

Table 1. Primers used for quantitative real-time PCR (qPCR). The forward (F) and reverse (R) primers for all the *Mus musculus* mRNAs or DNAs quantified by qPCR are indicated.

mRNA	Accession #	Forward (F) and Reverse (R) Primers
β-Actin	AK_145308	F: 5′- CCT AAG GCC AAC CGT GAA AA
		R: 5′- GAG GCA TAC AGG GAC AGC ACA
ULK2	NM_013881	F: 5′- GTG CTG TGG AAA TGG TTC AAT CTG
		R: 5′- CCT TGT GGT AGC GAT AAA CGA TGT C
GLUT4	BC_014282	F: 5′- CCA TTC CCT GGT TCA TTG TG
		R: 5′- GTT TTG CCC CTC AGT CAT TC
TFIIE	NM_026584	F: 5′- CAA GGC TTT AGG GGA CCA GAT AC
		R: 5′- CAT CCA TTG ACT CCA CAG TGA CAC
ACC1	AY_451393	F: 5′- CGG ACC TTT GAA GAT TTT GTC AGG
		R: 5′- GCT TTA TTC TGC TGG GTG AAC TCT C
ACC2	AY_451394	F: 5′- ATC ACC ACT CCT TCT GAC CCC ATC
		R: 5′- TCT CCA CAG CAA TCA CTC CCA C
FASN	NM_007988	F: 5′- CT GGA TAG CAT TCC GAA CCT G
		R: 5′- TTC ACA GCC TGG GGT CAT CTT TGC
Tfam	NM_009360	F: 5′- CAC TGG GAA ACC ACA GCA TAC AG
		R: 5′- GGA CAT CTG AGG AAA AGC CTT GC
eNOS	NM_008713	F: 5′- TGT CTG CGG CGA TGT CAC TAT G
		R: 5′- CGA AAA TGT CCT CGT GGT AGC G
PGC1α	NM_008904	F: 5′- CAC GAA AGG CTC AAG AGG GAT G
		R: 5′- CAC CAA AAA CTT CAA AGG GGT CTC
GSTA4	NM_010357	F: 5′- CGA TGG GAT GAT GCT GAC ACA
		R: 5′- CAC TGG GAA GTA ACG GGT TTT AGC
NQO-1	NM_008706	F: 5′- CCA TTC TGA AAG GCT GGT TTG AG
		R: 5′- CCT ATT CTG GAA AGG ACC GTT GTC
NRF-2	NM_010912	F: 5′- TGG AGC AAG TTT GGC AGG AG
		R: 5′- TGG GAA CAG CGG TAG TAT CAG C
COXII	NC_005089	F: 5′- TTT TCA GGC TTC ACC CTA GAT GA
		R: 5′- GAA GAA TGT TAT GTT TAC TCC TAC GAA TAT G

Table 2. Oligonucleotides for shRNA target sequences. GFP scrambled, ULK1 (#755), ULK1 (#768), ULK2 (#695), and Atg5 (#hp-2 from (Lum JJ 2005)) are targeted for knockdown.

Target for knockdown	shRNA sequence
GFP scrambled	5′-AAC GTA CGC GGA ATA CTT CGA-3′
ULK1 (#755)	5′-CCT GGT CAT GGA GTA TTG TAA-3′
ULK1 (#768)	5′-CGC TTC TTT CTG GAC AAA CAA-3′
ULK2	5′-CCA AAG ACT CTG CGA GTA ATA-3′
Atg5	5′-GGC ATT ATC CAA TTG GTT TA-3′

Bibliography

Abel ED, P. O., Kim JK, Kim YB, Boss O, Hadro E, Minnemann T, Shulman GI, Kahn BB (2001). "Adipose-selective targeting of the GLUT4 gene impairs insulin action in muscle and liver." Nature **8**: 729-733.

Achike FI, T. N., Wang H, Kwan CY. (2011). "Obesity, metabolic syndrome, adipocytes and vascular function: A holistic viewpoint." Clin Exp Pharmacol Physiol. **38**: 1-10.

Baerga R, Z. Y., Chen PH, Goldman S, Jin S. (2009). "Targeted deletion of autophagy-related 5 (atg5) impairs adipogenesis in a cellular model and in mice." Autophagy **5**: 1-13.

Beau I, M. M., Codogno P. (2011). "Autophagosomes and human diseases." Int J Biochem Cell Biol. **43**: 460-464.

Bittner CX, L. A., Ruminot I, Larenas V, Sotelo-Hitschfeld T, Gutiérrez R, Córdova A, Valdebenito R, Frommer WB, Barros LF. (2010). "High resolution measurement of the glycolytic rate." Front Neuroenergetics. **2**: 1-11.

Boudina S, D. A. E. (2005). "Mitochondrial Uncoupling: A Key Contributor to Reduced Cardiac Efficiency in Diabetes." Physiology **21**: 250-258.

Bournat JC, B. C. (2010). "Mitochondrial dysfunction in obesity." Curr Opin Endocrinol Diabetes Obes. **17**: 446-452.

Bursch W, H. K., Torok L, Marian B, Ellinger A, Hermann RS (2000). "Autophagic and apoptotic types of programmed cell death exhibit different fates of cytoskeletal filaments." J. Cell. Sci. **113**: 1189-1198

Camp HS, R. D., Leff T. (2002). "Adipogenesis and fat-cell function in obesity and diabetes " Trends Mol Med. **8**: 442-447.

Carlson, C. J., S. Koterski, et al. (2003). "Enhanced basal activation of mitogen-activated protein kinases in adipocytes from type 2 diabetes: potential role of p38 in the downregulation of GLUT4 expression." Diabetes **52**(3): 634-41.

Chan, E. Y., S. Kir, and S.A. Tooze (2007). "siRNA screening of the kinome identifies ULK1 as a multidomain modulator of autophagy. ." J Biol Chem **282**: 25464-25474.

Chang YY, N. T. (2009). "An Atg1/Atg13 complex with multiple roles in TOR-mediated autophagy regulation." Mol Biol Cell. **20**: 2004-2014.

Chen, X. H., Y. P. Zhao, et al (2010). "TNF-alpha induces mitochondrial dysfunction in 3T3-L1 adipocytes." Mol Cell Endocrinol **328**(1-2): 63-9.

Cheng Z, T. Y., White MF (2010). "Insulin signaling meets mitochondria in metabolism." Trends Endocrinol Metab. **21**: 589-598.

Circu ML, A. T. (2010). "Reactive oxygen species, cellular redox systems, and apoptosis. " Free Radic Biol Med. **15**: 749-762.

Curtis JM, G. P., Wright WS, Xu X, Foncea RE, Graham DW, Brestoff JR, Wiczer BM, Ilkayeva O, Cianflone K, Muoio DE, Arriaga EA, Bernlohr DA (2010). "Downregulation of adipose glutathione S-transferase A4 leads to increased protein carbonylation, oxidative stress, and mitochondrial dysfunction." Diabetes **59**: 1132-1142.

De Alvaro, C., T. Teruel, et al. (2004). "Tumor necrosis factor alpha produces insulin resistance in skeletal muscle by activation of inhibitor kappaB kinase in a p38 MAPK-dependent manner." J Biol Chem **279**(17): 17070-8.

De Pauw A, T. S., Raes M, Keijer J, Arnould T. (2009). "Mitochondrial (dys)function in adipocyte (de)differentiation and systemic metabolic alterations." Am J Pathol. **175**: 927-939.

Dunlop EA, H. D., Acosta-Jaquez HA, Fingar DC, Tee AR. (2011). "ULK1 inhibits mTORC1 signaling, promotes multisite Raptor phosphorylation and hinders substrate binding." Autophagy **7**: 737-747.

Egan D, K. J., Shaw RJ, Guan KL. (2011). "The autophagy initiating kinase ULK1 is regulated via opposing phosphorylation by AMPK and mTOR." autophagy **7**: 643-644.

Egan DF, S. D., Mihaylova MM, Gelino S, Kohnz RA, Mair W, Vasquez DS, Joshi A, Gwinn DM, Taylor R, Asara JM, Fitzpatrick J, Dillin A, Viollet B, Kundu M, Hansen M, Shaw RJ. (2011). "Phosphorylation of ULK1 (hATG1) by AMP-activated protein kinase connects energy sensing to mitophagy." Science **331**: 456-461.

Evans, J. L., I. D. Goldfine, et al. (2003). "Are oxidative stress-activated signaling pathways mediators of insulin resistance and beta-cell dysfunction?" Diabetes **52**(1): 1-8.

Ganley IG, L. d. H., Wang J, Ding X, Chen S, Jiang X. (2009). "ULK1.ATG13.FIP200 complex mediates mTOR signaling and is essential for autophagy." J Biol Chem. **284**: 12297-12305.

Gao, Z., D. Hwang, et al. (2002). "Serine phosphorylation of insulin receptor substrate 1 by inhibitor kappa B kinase complex." J Biol Chem **277**(50): 48115-21.

Gogvadze V, Z. B., Orrenius S. (2010). "The Warburg effect and mitochondrial stability in cancer cells." Mol Aspects Med. **31**: 60-74.

Goldman S, Z. Y., Jin S. (2010). "Autophagy and adipogenesis: implications in obesity and type II diabetes." Autophagy **6**: 179-181.

Grimsrud PA, P. M. S., Griffin TJ, Bernlohr DA (2007). "Carbonylation of adipose proteins in obesity and insulin resistance: identification of adipocyte fatty acid-binding protein as a cellular target of 4-hydroxynonenal." Mol. Cell. Proteomics **6**: 624-637.

Grimsrud PA, X. H., Griffin TJ, Bernlohr DA (2008). "Oxidative stress and covalent modification of protein with bioactive aldehydes." J. Biol. Chem. **283**: 21837-21841.

Gustafson, B. (2010). "Adipose tissue, inflammation and atherosclerosis." J Atheroscler Thromb. **17**: 331-341.

Hamanaka RB, C. N. (2010). "Mitochondrial reactive oxygen species regulate cellular signaling and dictate biological outcomes." Trends Biochem Sci. **35**: 505-513.

Hamm JK, e. J. A., Pilch PF, Farmer SR. (1999). "Role of PPAR gamma in regulating adipocyte differentiation and insulin-responsive glucose uptake." Ann N Y Acad Sci. **892**: 134-145.

Hara T, T. A., Kishi C, Iemura S, Natsume T, Guan JL, Mizushima N. (2008). "FIP200, a ULK-interacting protein, is required for autophagosome formation in mammalian cells." J Cell Biol. **181**: 497-510.

Hosokawa N, H. T., Kaizuka T, Kishi C, Takamura A, Miura Y, Iemura S, Natsume T, Takehana K, Yamada N, Guan JL, Oshiro N, Mizushima N. (2009). "Nutrient-dependent mTORC1 association with the ULK1-Atg13-FIP200 complex required for autophagy." Mol. Biol. Cell **20**: 1891-1991.

Hosokawa N, S. T., Iemura S, Natsume T, Hara T, Mizushima N. (2009). "Atg101, a novel mammalian autophagy protein interacting with Atg13." autophagy **5**: 973-979.

Jung CH, Jun CB, Ro SH, Kim YM, Otto NM, Cao J, Kundu M, Kim DH (2009). "ULK-mAtg13 complexes mediate mTOR signaling to the autophagy machinery." Mol. Biol. Cell **20**: 1992-2003.

Jung CH, Ro SH, Cao J, Otto NM, Kim DH (2010). "mTOR regulation of autophagy." FEBS Lett. **584**: 1287-1295.

Jung CH, Seo MC, Otto NM, Kim DH. (2011). "ULK1 inhibits the kinase activity of mTORC1 and cell proliferation." Autophagy **7**: 12112-1221.

Kahn, B. (1996). "Lilly lecture 1995. Glucose transport: pivotal step in insulin action." diabetes **45**: 1644-1654.

Kim J, K. M., Viollet B, Guan KL. (2011). "AMPK and mTOR regulate autophagy through direct phosphorylation of Ulk1." Nat Cell Biol. **13**: 132-141.

Kim JA, W. Y., Sowers JR (2008). "Role of mitochondrial dysfunction in insulin resistance." Circ. res. **102**: 401-414.

Klionsky DJ., A. H., Agostinis P et al. (2008). "Guidelines for the use and interpretation of assays for monitoring autophagy in higher eukaryotes." Autophagy **4**: 151-175.

Koves TR, U. J., Noland RC, Slentz D, Mosedale M, Ilkayeva O, Bain J, Stevens R, Dyck JR, Newgard CB, Lopaschuk GD, Muoio DM (2005). "Mitochondrial overload and incomplete fatty acid oxidation contribute to skeletal muscle insulin resistance." Cell Metab. **7**: 45-56.

Kovsan J, B. M., Tarnovscki T, Klöting N, Kirshtein B, Madar L, Shai I, Golan R, Harman-Boehm I, Schön MR, Greenberg AS, Elazar Z, Bashan N, Rudich A. (2011). "Altered autophagy in human adipose tissues in obesity." J Clin Endocrinol Metab. **96**: E268-E277.

Kundu M, L. T., Yang CY, Wu J, Zhao F, Zhang J, Selak MA, Ney PA, Thompson CB (2009). "Ulk1 plays a critical role in the autophagic clearance of mitochondria and ribosomes during reticulocyte maturation." Blood **112**: 1493-1502.

Lee SB, K. S., Lee J, Park J, Lee G, Kim Y, Kim JM, Chung J. (2007). "ATG1, an autophagy regulator, inhibits cell growth by negatively regulating S6 kinase." EMBO reports **8**: 360-365.

Levine B, K. G. (2008). "Autophagy in the pathogenesis of disease." Cell **132**: 27-42

Li, A. C. and C. K. Glass (2004). "PPAR- and LXR-dependent pathways controlling lipid metabolism and the development of atherosclerosis." J Lipid Res **45**(12): 2161-73.

Liang H, W. W. (2006). "PGC-1alpha: a key regulator of energy metabolism." Adv Physiol Educ. **30**: 145-151.

Liao W, N. M., Yoshizaki T, Favelyukis S, Patsouris D, Imamura T, Verma IM, Olefsky JM. (2007). "Suppression of PPAR-gamma attenuates insulin-stimulated glucose uptake

by affecting both GLUT1 and GLUT4 in 3T3-L1 adipocytes." Am J Physiol Endocrinol Metab. **293**: E219-E227.

Lin J, P. K., Della-Fera MA, Baile CA. (2004). "Evaluation of adipocyte apoptosis by laser scanning cytometry." Int J Obes Relat Metab Disord. **28**: 1535-1540.

Lobo S, W. B., Smith AJ, Hall AM, Bernlohr DA (2007). "Fatty acid metabolism in adipocytes: functional analysis of fatty acid transport proteins 1 and 4." J.Lipid Res. **48**: 609-620.

Löffler AS, A. S., Dieterle AM, Keppeler H, Franz-Wachtel M, Kundu M, Campbell DG, Wesselborg S, Alessi DR, Stork B. (2011). "k1-mediated phosphorylation of AMPK constitutes a negative regulatory feedback loop." Autophagy **7**: 696-706.

Lowell, B. B. a. G. I. S. (2005). "Mitochondrial dysfunction and type 2 diabetes." Science **307**: 384-387.

Lum JJ, B. D., Kong M, Harris MH, Li C, Lindsten T, Thompson CB (2005). "Growth factor regulation of autophagy and cell survival in the absence of apoptosis." Cell **120**: 237-248.

Marcelin G, C. S. J. (2010). "Contributions of adipocyte lipid metabolism to body fat content and implications for the treatment of obesity." Curr Opin Pharmacol. **10**: 588-593.

Medina-Gomez G, G. S., Vidal-Puig A. (2007). "Adipogenesis and lipotoxicity: role of peroxisome proliferator-activated receptor gamma (PPARgamma) and PPARgammacoactivator-1 (PGC1)." Public Health Nutr. **10**: 1132-1137.

Mercer CA, K. A., Dennis PB (2009). "A novel, human Atg13 binding protein, Atg101, interacts with ULK1 and is essential for macroautophagy." **5**: 649-662.

Mizushima N, L. B., Cuervo AM, Klionsky DJ (2008). "Autophagy fights disease through cellular self-digestion." Nature **451**: 1069-1075

Mizushima N, Y. A., Hatano M, Kobayashi Y, Kabeya Y, Suzuki K, Tokuhisa T, Ohsumi Y, Yoshimori T. (2001). "Dissection of autophagosome formation using Apg5-deficient mouse embryonic stem cells." J. Cell. Biol. **152**: 657-667.

Mizushima, N. a. T. Y. (2007). "How to interpret LC3 immunoblotting." Autophagy **3**: 542-545.

Mizushima, N. (2010). "The role of the Atg1/ULK1 complex in autophagy regulation " Curr Opin Cell Biol. **22**: 132-139.
Nieto-Vazquez, I., S. Fernandez-Veledo, et al. (2008). "Insulin resistance associated to obesity: the link TNF-alpha." Arch Physiol Biochem **114**(3): 183-94.

Nishida Y, A. S., Fujitani K, Yamaguchi H, Mizuta T, Kanaseki T, Komatsu M, Otsu K, Tsujimoto Y, Shimizu S. (2009). "Discovery of Atg5/Atg7-independent alternative macroautophagy. ." Nature **461**: 654-658.

Nishikawa T, A. E. (2007). "Impact of mitochondrial ROS production in the pathogenesis of diabetes mellitus and its complications." Antioxid Redox Signal. **9**: 343-353.

Ost A, S. K., Ruishalme I, Brännmark C, Franck N, Krook H, Sandström P, Kjolhede P, Strålfors P. (2010). "Attenuated mTOR signaling and enhanced autophagy in adipocytes from obese patients with type 2 diabetes." Mol. Med. **16**: 235-246

Pauw AD, T. S., Raes M, Keijer J, Arnould T (2009). "Mitochondrial (Dys) function in Adipocyte (De) differentiation and Systemic Metabolic Alterations." Am. J. Path. **175**: 927-939.

Piantadosi CA, S. H. (2006). "Mitochondrial transcription factor A induction by redox activation of nuclear respiratory factor 1." J. Biol. Chem. **281**: 324-333.

Rigoulet M, Y. E., Devin A. (2011). "Mitochondrial ROS generation and its regulation: mechanisms involved in H(2)O(2) signaling." Antioxid Redox Signal. **14**: 459-468.

Rosen ED, S. B. (2006). "Adipocytes as regulators of energy balance and glucose homeostasis." Nature **444**: 847-853.

Saltiel AR, K. C. (2001). "Insulin signalling and the regulation of glucose and lipid metabolism." Nature **414**: 799-806.

Scherz-Shouval R, E. Z. (2007). "ROS, mitochondria and the regulation of autophagy." Trends Cell Biol. **17**: 422-427.

Scott RC, J. G., Neufeld TP. (2007). "Direct induction of autophagy by Atg1 inhibits cell growth and induces apoptotic cell death." Curr Biol. **17**: 1-11.

Shaw RJ, K. M., Bardeesy N, Hurley RL, Witters LA, DePinho RA, Cantley LC. (2004). "The tumor suppressor LKB1 kinase directly activates AMP-activated kinase and regulates apoptosis in response to energy stress." Proc Natl Acad Sci U S A. **101**: 3329-3335.

Shimada Y, K. H., Kawagoe S, Aoki K, Kaneshiro E, Shimizu H, Eto Y, Ida H, Ohashi T. (2011). "Endoplasmic reticulum stress induces autophagy through activation of p38 MAPK in fibroblasts from Pompe disease patients carrying c.546G>T mutation." Mol Genet Metab. **104**: 566-573.

Shoshan-Barmatz V, D. P. V., Zweckstetter M, Raviv Z, Keinan N, Arbel N. (2010). "VDAC, a multi-functional mitochondrial protein regulating cell life and death." Mol Aspects Med. **31**: 227-285.

Singh R, K. S., Wang Y, Xiang Y, Novak I, Komatsu M, Tanaka K, Cuervo AM, Czaja MJ (2009). "Autophagy regulates lipid metabolism." Nature **458**: 1131-1135

Singh R, X. Y., Wang Y, Baikati K, Cuervo AM, Luu YK, Tang Y, Pessin JE, Schwartz GJ, Czaja MJ (2009). "Autophagy regulates adipose mass and differentiation in mice." J. Clin. Invest. **119**: 3329-3339

sokawa N, H. T., Kaizuka T, Kishi C, Takamura A, Miura Y, Iemura S, Natsume T, Takehana K, Yamada N, Guan JL, Oshiro N, Mizushima N. (2009). "Nutrient-dependent mTORC1 association with the ULK1-Atg13-FIP200 complex required for autophagy." Mol Biol Cell. **20**: 1981-1991.

Student AK, H. R., Lane MD (1980). "Induction of fatty acid synthase synthesis in differentiating 3T3-L1 preadipocytes." J Biol Chem. **255**: 4745-4750.

Surwit RS, K. C., Cochrane C, McCubbin JA, Feinglos MN (1988). "Diet-induced type II diabetes in C57BL/6J mice." Diabetes **37**: 1163-1167.

Tanida I, U. T., Kominami E. (2004). "LC3 conjugation system in mammalian autophagy." Int J Biochem Cell Biol. **36**: 2503-2518.

Tontonoz P, H. E., Spiegelman BM. (1994). "Stimulation of adipogenesis in fibroblasts by PPAR gamma 2, a lipid-activated transcription factor." Cell **79**: 1147-1156.

Tontonoz P, S. B. (2008). "Fat and Beyond: The Diverse Biology of PPARγ." Annu. Rev. Biochem. **77**: 289-312.

Trayhurn, P. (2007). "Adipocyte biology." Obes Rev. **1**: 41-44.

Ueda S, M. H., Nakamura H, Tanaka T, Ueno M, Yodoi J. (2002). "Redox control of cell death." Antioxid Redox Signal. **4**: 405-414.

Um SH, F. F., Watanabe M, Picard F, Joaquin M, Sticker M, Fumagalli S, Allegrini PR, Kozma SC, Auwerx J, Thomas G. (2004). "Absence of S6K1 protects against age- and diet-induced obesity while enhancing insulin sensitivity." Nature **431**: 200-205.

Wang CH, W. C., Wei YH. (2010). "Mitochondrial dysfunction in insulin insensitivity: implication of mitochondrial role in type 2 diabetes." Ann N Y Acad Sci. **1201**: 157-165.

Weidberg H, S. E., Elazar Z. (2011). "Biogenesis and cargo selectivity of autophagosomes." Annu Rev Biochem. **80**.

Wu M, N. A., Swift AL, Moran R, Tamagnine J, Parslow D, Armistead S, Lemire K, Orrell J, Teich J, Chomicz S, Ferrick DA (2007). "Multiparameter metabolic analysis reveals a close link between attenuated mitochondrial bioenergetic function and enhanced glycolysis dependency in human tumor cells." Am J Physiol Cell Physiol. **292**: C125-136.

Xu X, A. E. (2009). "Qualitative determination of superoxide release at both sides of the mitochondrial inner membrane by capillary electrophoretic analysis of the oxidation products of triphenylphosphonium hydroethidine." Free Radic Biol Med. **46**: 905-913.

Yang, J., Y. Park, et al. (2009). "Feed-forward signaling of TNF-alpha and NF-kappaB via IKK-beta pathway contributes to insulin resistance and coronary arteriolar dysfunction in type 2 diabetic mice." Am J Physiol Heart Circ Physiol **296**(6): H1850-8.

Yorimitsu T, N. U., Yang Z, Klionsky DJ (2006). "Endoplasmic reticulum stress triggers autophagy." J. Biol. Chem. **281**: 30299-30304

Yuan, M., N. Konstantopoulos, et al. (2001). "Reversal of obesity- and diet-induced insulin resistance with salicylates or targeted disruption of Ikkbeta." Science **293**(5535): 1673-7.

Zhang HH, H. J., Düvel K, Boback B, Wu S, Squillace RM, Wu CL, Manning BD (2009). "Insulin stimulates adipogenesis through the Akt-TSC2-mTORC1 pathway." PLoS One **4**: e6189.

Zhang, J., Z. Gao, et al. (2008). "S6K directly phosphorylates IRS-1 on Ser-270 to promote insulin resistance in response to TNF-(alpha) signaling through IKK2." J Biol Chem **283**(51): 35375-82.

Zhang Y, G. S., Baerga R, Zhao Y, Komatsu M, Jin S. (2009). "Adipose-specific deletion of autophagy-related gene 7 (atg7) in mice reveals a role in adipogenesis." Proc. Natl. Acad. Sci. USA **106**: 19860-19865.

Zhou L, Z. J., Fang Q, Liu M, Liu X, Jia W, Dong LQ, Liu F. (2009). "Autophagy-mediated insulin receptor down-regulation contributes to endoplasmic reticulum stress-induced insulin resistance." Mol. Pharmacol. **76**: 596-603.

Appendix : CURRICULUM VITAE

Name : **Seung-Hyun Ro**
Birth : Male, Born on 1976 in Daejon, Korea
Major Fields : Biomedical Sciences
Contact Info : Phone : +1-612-615-5379
E-mail : shro1129@gmail.com

Education :

2011	**Ph.D.** in Biochemistry, Molecular Biology and Biophysics, University of Minnesota, Minneapolis, MN, USA Thesis : Distinct Functions of Autophagy Kinases ULK1 and ULK2 in Adipogenesis and Adipocyte Metabolism (Advisor : Dr. Do-Hyung Kim)
2001	**M.S.** in Biological Sciences, KAIST, Daejon, Korea Thesis : Transcriptional Sequencing Activity of T7 RNA Polymerase Mutants (Advisor : Dr. Changwon Kang)
1999 – 2000	Exchange Student in Biological Sciences, University of British Columbia, Vancouver, Canada
1999	**B.S.** in Chemistry, Minor in Biological Sciences, KAIST, Daejon, Korea Thesis : Synthesis of Contrast Agents for Tumor-diagnostic Magnetic Resonance Imaging (Advisor : Dr. Young-Hwan Jang)

Professional Experiences :

2012 – Pres.	Postdoctoral Research Associate, Department of Pathology & Laboratory Medicine, Cornell University Weill Medical College, New York, NY, USA (Dr. Jihye Paik)
2006 – 2011	Graduate Research Assistant, Department of Biochemistry, Molecular Biology and Biophysics, University of Minnesota, Minneapolis, MN, USA (Dr. Do-Hyung Kim)
2008	Teaching Assistant in Biology Program, University of Minnesota, Minneapolis, MN, USA (Dr. Rick Peifer)
2005	Junior Researcher, Department of Pharmacy, Pusan National University, Pusan, Korea (Dr. Nam-Chul Ha)
2001 – 2003	Teaching Assistant in Molecular Genetics and Microbiology Program, The University of Texas at Austin, TX, USA (Dr. Susan Barth)
2000 – 2001	Graduate Research Assistant in Biological Sciences, KAIST, Daejon, Korea (Dr. Changwon Kang)

Publications :

5. **Ro SH**, Jung CH, Wright W, Xu X, Kim YM, Yun YS, Seo MS, Arraga EA, Bernlohr DA, Kim DH. Distinct functions of autophagy kinases ULK1 and ULK2 in adipogenesis and adipocyte metabolism. *Autophagy*, 2011 Submitted.
4. Jung CH, **Ro SH**, Cao J, Otto NM, Kim DH. mTOR regulation of autophagy. *FEBS Lett.* 584: 1287-1295, 2010 Invited review
3. Bandhakavi S, Kim YM, **Ro SH**, Xie HW, Griffin TJ, Kim DH. Proteomic and downstream analysis reveals a novel role for mTOR in regulation of DNA-damage response pathways. *Mol. Cell. Proteomics* 9: 403-414, 2010
2. Jung CH, Jun CB, **Ro SH**, Kim YM, Otto NM, Cao J, Kundu M, Kim DH. ULK-Atg13-FIP200 complexes mediate mTOR signaling to the autophagy machinery. *Mol. Biol. Cell* 20: 1992-2003, 2009
1. **Ro SH**, Ha NC. High-level production and initial crystallization of a Fe65 domain. **J. of Life Sci.* 17:18-23, 2007 (*Korean Journal)

Extramural Presentations :

3. **Ro SH**, Kim DH. Role of adipose autophagy in insulin resistance. Minnesota Obesity Center research conference 2011. Minnespolis, MN. Feb. 1, 2011 – Invited poster session
2. **Ro SH**, Jung CH, Kim YM, Wright W, Bernlohr DA, Kim DH. Roles of the ULK1-Atg13 complex in adipose autophagy, differentiation, and metabolism. 70th annual meeting of American Diabetes Association. Orlando, FL. Jun. 25-29, 2010 – Oral presentation
1. Jung CH, **Ro SH**, Cao J, Otto NM, Kim DH. ULK1 is a negative regulator of mTOR complex-1 and cell growth. Gordon research conference, Autophagy in stress, development & disease. Lucca, Italy. Apr. 25-30, 2010 – Poster presentation

Awards and Honors :

2010	Travel Grants for Trainees in Diabetes Research, Center for Diabetes Research, University of Minnesota, USA
2008	Teaching Assistant Scholarship, Department of Biology, University of Minnesota, USA
2001 – 2003	Teaching Assistant Scholarship, Department of Microbiology, The University of Texas at Austin, USA
2001	Dean's Excellency Award from Dean of Biological Sciences Program, The University of Texas at Austin, USA
2000 – 2001	Graduate Scholarship, Ministry of Science and Technology, Korea